



1 Drainage reorganization and divide migration induced by the excavation of the Ebro basin
2 (NE Spain)

3

4 Arnaud Vacherat¹, Stéphane Bonnet¹, Frédéric Mouthereau¹

5

6 ¹Géosciences Environnement Toulouse (GET), Université de Toulouse, UPS, Univ. Paul
7 Sabatier, CNRS, IRD, 14 av. Edouard Belin, F-31400 Toulouse, France

8

9 *Correspondance to:* Arnaud Vacherat (arnaud.vacherat@get.omp.eu)

10

11 **Abstract**

12

13 Intracontinental endorheic basins are key elements of source-to-sink systems as they preserve
14 sediments eroded from surrounding catchments. Drainage reorganization in such a basin has
15 strong implications on the sediment routing system and on the landscape evolution at a cratonic
16 scale.

17

18 The Ebro and Duero basins in the north Iberian plate represent two foreland basins, which were
19 filled in relation with the growing of surrounding compressional orogens as the Pyrenees and
20 the Cantabrian mountains to the north, the Iberian and Central Ranges to the south, and the
21 Catalan Coastal Range to the east. They were once connected as endorheic basins in the Early
22 Oligocene. By the end of the Miocene, they were disconnected and started to flow into the
23 Mediterranean Sea and the Atlantic Ocean, respectively, in a post-orogenic context.

24 Although these two hydrographic basins recorded similar histories, they are characterized by
25 very different morphologic features. The Ebro basin is highly excavated, whereas the Duero
26 basin is well preserved and may be considered as almost still endorheic.

27

28 These two bordering basins then show contrasting preservation states of their endorheic stages
29 and represent an ideal natural laboratory to study what factors (internal / external) control
30 drainage divide mobility, and drainage network and landscape evolution in post-orogenic
31 basins.

32 To that aim, we use field and map observations and we apply the Chi-analysis of river profiles
33 across the divide along the boundary between the Ebro and Duero drainage basins in the
34 Northern Iberian Peninsula to evaluate the migration of their divide.



35

36 We show here that contrasting excavation of the Ebro and Duero basins drives a reorganization
37 of their drainage network through a series of captures and resulted in the southwestward
38 migration of their main drainage divide. Fluvial captures have strong impact on drainage areas,
39 fluxes, and so on incision capacity, especially for the captured basin.

40 Thus, we conclude that drainage reorganization, and capture of the Duero rivers by the Ebro
41 ones, independently from tectonics and climate, enable endorheism in the Duero basin due to
42 drainage area loss.

43

44 **1. Introduction**

45

46 Landscapes subjected to contrasted erosion rates between adjacent drainage basins shows a
47 migration of their drainage divide toward the area of lower erosion rates (Bonnet, 2009). This
48 is the case for example in mountain ranges characterized by gradients in precipitation rates due
49 to orography, once landscapes are in a transient state and are not adjusted to precipitation
50 differences (Bonnet, 2009). It can also occur when drainage reorganized in response to capture
51 (Yanites et al., 2013; Willett et al., 2014). River capture actually drives a discrete drop in the
52 location of drainage divide (Prince et al. 2011) but also drives a wave of erosion in the capture
53 reach (Yanites et al., 2013) that may also impact divide position. Historically, migration of
54 divides has been inferred for instance by changes in the provenance of sediments stored in
55 sedimentary basins (*e.g.* Kuhlemann et al., 2001). It is however a process that is generally very
56 difficult to document in erosional landscapes. Recent developments have been performed to
57 infer divide migration from landscape analysis (Bonnet, 2009; Castelltort et al., 2012; Willett
58 et al., 2014; Whipple et al., 2017). Among them the recently-developed Chi-method for
59 analyzing longitudinal profiles of rivers (Perron and Royden, 2013) is based on the recognition
60 of disequilibrium along river profiles, disequilibrium being defined by the departure from an
61 ideal equilibrium shape. The application of this method to some natural landscapes, also
62 verified by similar analyses performed on numerically-simulated ones, has allowed to
63 demonstrate contrasts in the equilibrium state of rivers across divide and then to infer their
64 migration (Willett et al., 2014). The applicability of this method is however limited to settings
65 where the response time of rivers is larger compared to the rate of divide migration, so they can
66 actually show disequilibrium in their longitudinal profiles (Whipple et al., 2017).

67



68 In this study, we use field observations and we apply the Chi-analysis of river profiles across
69 divide along the boundary between the Ebro and Duero drainage basins in the Northern Iberian
70 Peninsula to evaluate the migration of their divide. These two drainage basins show geological
71 and geomorphological evidences indicating that they record very contrasted erosional histories
72 during the Neogene. They went through a long endorheic stage since the Early Oligocene before
73 being opened toward the Atlantic Ocean (Duero) or the Mediterranean Sea (Ebro) during the
74 Late Miocene, in a post-orogenic context. The Ebro basin's opening led to important unfilling
75 and excavation (Garcia-Castellanos et al., 2003), whereas opening of the Duero basin did not
76 drive excavation of its upstream part, that can then be considered as almost still endorheic
77 (Antón et al., 2012). The Duero River shows a pronounced knickpoint (knickzone) in the
78 downstream end of its longitudinal profile that limits an upstream domain of high mean
79 elevation (~800 m) where the sedimentary filling of its endorheic stage is relatively well
80 preserved. These two bordering basins are then characterized by contrasting preservation states
81 of their endorheic stages and represent an ideal natural laboratory to study what factors control
82 drainage divide mobility, and drainage network and landscape evolution in post-orogenic
83 basins.

84

85 We show here that contrasting excavation between the Ebro and Duero basins drives a
86 reorganization of their drainage network through a series of captures and resulted in the
87 southwestward migration of their main drainage divide. Fluvial captures have strong impact on
88 drainage areas, fluxes, and so on incision capacity, especially for the captured basin. Thus, we
89 conclude that drainage reorganization, and capture of the Duero rivers by the Ebro ones,
90 independently from tectonics and climate, enable endorheism in the Duero basin due to drainage
91 area loss.

92

93 **2. Geological setting**

94

95 **2.1 The Ebro and Duero basins**

96

97 The Ebro and Duero basins represent two hydrographic basins covering the northern part of the
98 Iberian Peninsula (Fig. 1). The bedrock of the Ebro and Duero drainage basins mainly consists
99 on Cenozoic deposits, and Mesozoic and Paleozoic rocks in their headwaters (Fig. 2). They
100 used to form a unique foreland basin during the Cenozoic, connected in the Rioja Trough
101 (Mikeš, 2010), due to flexural subsidence related to the orogenic growth of their surroundings :



102 the Pyrenees and the Cantabrian mountains to the north (Pulgar et al., 1999), the Iberian and
103 Central Ranges to the south (Guimerà et al., 2004; De Vicente et al., 2007), and the Catalan
104 Coastal Range (CCR) to the east (López-Blanco et al., 2000 ; Salas et al., 2001), during collision
105 between Iberia and Europe since the Late Cretaceous.

106

107 Since early stage of collision, the Ebro and Duero basins were essentially filled by siliciclastic
108 and carbonated alluvial sediments, and opened toward the Bay of Biscay (Alonso-Zarza et al.,
109 2002). During the Late Eocene – Early Oligocene, uplift in the Western Pyrenees
110 (Puigdefàbregas et al., 1992) led to the closure of the Ebro and Duero basins and to
111 continentalization in an endorheic setting (Costa et al., 2010). The center of these two basins
112 became long-lived lakes filled with lacustrine, sandy, and evaporitic deposits from the
113 Oligocene to the Miocene (Riba et al., 1983; Alonso-Zarza et al., 2002; Pérez-Rivarés et al.,
114 2002, 2004; Garcia-Castellanos et al., 2003; Garcia-Castellanos, 2006; Larrasoña et al., 2006;
115 Vázquez-Urbez et al., 2013). Opening of the Ebro basin through the Catalan Coastal Range
116 toward the Mediterranean Sea to the East occurred during the Late Miocene, leading to
117 important unfilling and excavation recorded throughout the basin (Fillon and Van der Beek,
118 2012; Fillon et al., 2013; Garcia-Castellanos and Larrasoña, 2015). However, its exact timing
119 and its relation to the Messinian Salinity Crisis, as well as what processes is underlying this
120 opening, has long been debated (Coney et al., 1996; Garcia-Castellanos et al., 2003; Babault et
121 al., 2006; Urgeles et al., 2010; Garcia-Castellanos and Larrasoña, 2015). By contrast, incision
122 in the Duero basin appears very limited, although opening through the Iberian Massif toward
123 the Atlantic Ocean to the west occurred progressively from west to east by river capture, from
124 the Late Miocene-Early Pliocene to the Late Pliocene-Early Pleistocene (Martín-Serrano,
125 1991). The upstream Duero basin is characterized nowadays by a low relief topography (Fig.
126 1) at 700-800 m above sea level to the west, and at 1000-1100 m a.s.l. to the north, northeast,
127 and to the east in the Almazan subbasin, close to the divide with the Ebro basin.

128 In the following, we review the geological evolution of the different domains that constitute
129 today the drainage divide between the Ebro and Duero drainage basins as well as evidences for
130 drainage mobility already recognized in previous studies. The current Ebro and Duero drainage
131 networks are separated by a divide running from the Cantabrian belt to the NW, toward the SE
132 in the Iberian Range (Figs. 1, 2, 3). The easternmost part of the Duero river is opposed to the
133 Ebro tributaries that are the Jalon, Huecha, Queiles, Alama, Cidacos, Iregua, and Najerilla
134 rivers, whereas the Arlanzón and Pisuerga rivers (Duero tributaries) are opposed to the
135 Najerilla, Tiron, Oca, and Rudron rivers, and to the westernmost part of the Ebro river (Fig. 3).



136 The Northeastern part of the Duero basin (the easternmost Duero river, the Arlanzon and
137 Pisuerga rivers) mainly consists in broad flat valleys characterized by low incision depth, with
138 low-gradient streams dominated by concave longitudinal profiles (Antón et al., 2012, 2014).
139 By contrast, the western part of the Ebro basin is characterized by more incised valleys,
140 especially in the Cantabrian and in the Cameros – Iberian Range domains, with more complex
141 longitudinal profiles (knickpoints, remnants of high elevated surfaces).

142

143 2.2 Geology and drainage divide in The Iberian Range

144

145 The Iberian Range (Figs. 2, 4) is a double vergent fold-and-thrust belt resulting from inversion
146 of rift-related Mesozoic basins since the Late Cretaceous in response to Iberia – Europe
147 convergence (Salas et al., 2001; Guimerà et al., 2004; Martín-Chivelet et al., 2002). It is divided
148 into two NW-SE orientated branches, the Aragonese and the Castillian branches, separated by
149 the Tertiary Almazan subbasin, which results from flexural subsidence due to thrusting in the
150 Iberian Range (Bond, 1996). The Almazan subbasin is connected to the Duero basin since the
151 Early Miocene (Alonso-Zarza et al., 2002).

152 The Iberian Range is essentially made of marine carbonates to continental clastic sediments
153 from the Late Permian to the Albian, covering a Hercynian basement. The Cameros subbasin
154 to the NW represents an Early Cretaceous highly subsiding trough almost exclusively filled by
155 continental siliciclastic deposits (Martín-Chivelet et al., 2002 and references therein; Del Rio
156 et al., 2009). Shortening is recorded up to the Early Miocene, and accomodated by hercynian
157 inherited NW-SE structures (Gutiérrez-Elorza and Gracia, 1997; Guimerà et al., 2004;
158 Gutiérrez-Elorza et al., 2002). This event is responsible for the opening of the Calatayud basin
159 in the Aragonese branch during the Early Miocene, as dextral and inverse deformations are
160 recorded on its southern margin (Daroca area) (Colomer and Santanach, 1988). It is followed
161 during the Pliocene and the Pleistocene, by pulses of extensive deformations leading to fault
162 reactivations in the Calatayud basin, and to the formation of new depressions, as the Daroca,
163 Munébrega, Gallocanta, and Jiloca grabens (Fig. 4; Colomer and Santanach, 1988; Gutiérrez-
164 Elorza et al., 2002; Capote et al., 2002). This is also outlined by the occurrence of breccias and
165 glaciais levels deposited in the Daroca and Jiloca grabens from the Late Pliocene to the Early
166 Pleistocene (Gracia, 1992, 1993a; Gracia and Cuchi, 1993; Gutiérrez-Santolalla et al., 1996).
167 These Neogene troughs are filled by continental deposits and pediments, up to the Quaternary
168 (Fig. 4).



169 The Neogene tectonic history of the Iberian Range is characterized by tectonic pulses
170 intercalated with quiescence periods responsible for the formation of erosion surfaces from the
171 Early Miocene to the Late Pliocene – Early Pleistocene (Gutiérrez-Elorza and Gracia, 1997).
172 These surfaces are highly reworked and/or deformed due to subsequent tectonic activity, except
173 for the youngest one, which appears only affected by surface processes as fluvial incision
174 (Gutiérrez-Elorza and Gracia, 1997).

175

176 Uplift in the Iberian Range and Cameros basin resulted in the isolation of the Almazan subbasin
177 (Alonso-Zarza et al., 2002) separating the Duero from the Ebro, whereas they are still connected
178 to the Northwest, especially through the proto-Rioja trough (Mikeš, 2010). Compression in the
179 Northwest Iberian Range continues and the inverted Cameros basin is deformed as a large
180 anticline that plunges to the W-NW, finally connecting to the Cantabrian domain through the
181 Rioja trough in the Late Oligocene. This disconnects the Ebro from the Duero basins, localizing
182 the divide further East from its present-day location (Mikeš, 2010). During the Early Miocene,
183 the Almazan subbasin, initially connected to the Ebro, became connected to the Duero basin
184 (Alonso-Zarza et al., 2002), whereas in the Iberian Range, the formation of the Calatayud basin
185 separated the Ebro from the Almazan-Duero basin.

186 The Almazan subbasin (Figs. 2, 4) is currently partly drained by the Ebro drainage network and
187 especially by the Jalon river (Fig. 4). To capture this domain, the Jalon river had to cross the
188 Mesozoic and Neogene strata and the two Paleozoic ridges of the Aragonese branch of the
189 Iberian Range. According to morpho- and chrono-stratigraphic evidences, the Jalon river
190 captured the Calatayud basin after the Messinian (Gutiérrez-Santolalla et al., 1996). Its
191 tributary, the Jiloca river, captured the Daroca graben to the east during the Late Pliocene –
192 Early Pleistocene, and the Jiloca graben, to the southeast, from the Early to Late Pleistocene
193 (Gutiérrez-Santolalla et al., 1996). It is finally followed by the capture of the Munébraga graben
194 to the southwest, by the Jalon river (Gutiérrez-Santolalla et al., 1996), toward the easternmost
195 part of the Almazan subbasin.

196

197 2.3 Geology and drainage divide in the Rioja trough and the Bureba high

198

199 The Rioja trough (Figs. 2, 5) recorded important subsidence, especially during the Cenozoic (>
200 5 km), related to compression and thrusting on its borders (Jurado and Riba, 1996). As thrusting
201 initiated in the Pyrenean-Cantabrian belt and in the Iberian Range and Cameros basin, the Rioja
202 trough became an important bypass domain connecting the Ebro and Duero basins. During the



203 Paleocene, a marine environment took place, becoming more and more continental up to the
204 Late Eocene. Thrusting continued during the Oligocene resulting in the formation of an
205 anticline connecting the Cantabrian domain and the Cameros inverted basin. This morphologic
206 high (the Bureba anticline) located in the center of the area is supposed to have disconnected
207 the Duero and Ebro basins (Mikeš, 2010), as suggested by the repartition of detritic alluvial
208 fans on both sides of this structure (Muñoz-Jiménez and Casas-Sainz, 1997; Villena et al.,
209 1996). During the Miocene, deformations ceased as evidenced by the deposition of undeformed
210 middle Miocene to Holocene strata. The Bureba anticline is cored by Albian strata and topped
211 by Santonian limestones and Oligocene conglomerates controlling the location of the current
212 main drainage divide between the Ebro and Duero river networks.

213 The western part of the Rioja trough to the west of the NE-SW directed branch of the Bureba
214 anticline (Fig. 5), used to be drained toward the Duero basin since the Oligocene (Mikeš, 2010).
215 The westward migration of the divide to its current location is thought to have occurred in
216 several steps as shown by the occurrence of remnants of escarpments during the Late Miocene
217 - Pliocene (Mikeš, 2010). Once the eastern branch of the Bureba anticline has been incised, the
218 Ebro tributaries captured the western part of the Rioja trough, up to the E-W branch of the
219 Bureba anticline to the southwest, from the Late Miocene to the Pliocene. Finally, the upper
220 reach of the Jordan (Ubierna - Duero) river to the west has been captured by the Homino (Oca
221 - Ebro) river during the Quaternary (Fig. 5). The Bureba area is then considered as dynamically
222 stable as witnessed by the good superposition of the current streams and Quaternary fluvial
223 deposits (Mikeš, 2010).

224

225 2.4 Climatic evolution

226

227 Climate exerts a major control on valley incision, sediment discharge, and on the evolution of
228 drainage network (Bonnet, 2009; Whitfield and Harvey, 2012; Stange et al., 2014). The mean
229 annual precipitation map for the North Iberian Peninsula (Hijmans et al., 2005) shows a similar
230 pattern for both the Ebro and Duero basins as they record very low precipitation, associated to
231 global subarid conditions, with the exception of the Cameros basin that record a slightly higher
232 precipitation rate (Fig. 6). There is a strong contrast to the north, toward the Mediterranean Sea
233 and the most elevated areas in the Cantabrian and Pyrenean belts, where precipitations
234 drastically increase.

235 The paleoclimatic evolution from the Late Cretaceous to the Neogene is linked both with the
236 effects of surrounding mountains uplift, and with the latitudinal variation due to the rotation of



237 Iberia, from 30°N in the Cretaceous to ~40°N during Late Neogene times. The hot-humid
238 tropical climate of the Late Cretaceous became more and more dry and arid from the Paleocene
239 to the Middle Miocene (López-Martínez et al., 1986), favouring the development of endorheic
240 lakes (García-Castellanos, 2006). During the Middle-Late Miocene and Early Pliocene, the
241 northern Iberia recorded more humid and seasonal conditions (Calvo et al., 1993; Alonso-Zarza
242 and Calvo, 2000) with alternations of cold-wet and hot-dry periods (Bessais and Cravatte, 1988;
243 Rivas-Carballo et al., 1994; Jiménez-Moreno et al., 2010). More humid and colder conditions
244 then took place in the Late Pliocene, characterized by dry glacial periods and humid
245 interglacials (Suc and Popescu, 2005; Jiménez-Moreno et al., 2013). Climatic contrasts
246 increased, triggering intense glaciers fluctuations in the surrounding mountain ranges during
247 the Lower-Middle Pleistocene transition (1.4-0.8 Ma) (Moreno et al., 2012; Duval et al., 2015;
248 Sancho et al., 2016), and throughout the Late Pleistocene period, which record important glacial
249 / interglacial oscillations, as evidenced by pollen identification (Suc and Popescu, 2005;
250 Jiménez-Moreno et al., 2010, 2013; Barrón et al., 2016; García-Ruiz et al., 2016) and
251 speleothem studies (Moreno et al., 2013; Bartolomé et al., 2015).

252 Glaciers are considered as the most efficient erosion tool in continental environment. They are
253 likely to influence drainage divide migration (Brocklehurst and Whipple, 2002). There is large
254 evidence of glaciers development especially for the Late Pleistocene in the Pyrenees (Delmas
255 et al., 2009; Nivière et al., 2016; García-Ruiz et al., 2016), in the Cantabrian belt (Serrano et
256 al., 2013, 2016; García-Ruiz et al., 2016), and in the Central Range (Palacios et al., 2011, 2012;
257 García-Ruiz et al., 2016). However, although numerous moraines have been mapped throughout
258 the Iberian Range (Ortigosa, 1994; García-Ruiz et al., 1998; Pellicer and Echeverría, 2004),
259 there is no evidence of U-shaped valleys and because of the lack of very high elevated massifs
260 (>2500 m), the occurrence of active ice tongue is considered as limited, if not precluded
261 (García-Ruiz et al., 2016).

262

263 **3. Morphometric analyses**

264

265 As mentioned above, it has already been shown that the Jalon and Homino rivers, which belong
266 to the Ebro basin, have recently captured parts of the Duero basin in the Iberian Range and in
267 the Rioja trough, respectively (Gutiérrez-Santolalla et al., 1996; Mikeš, 2010). Such evolution
268 has been recorded by the occurrence of geomorphological markers as wind gaps and elbows of
269 captures, as well as by the presence of knickpoints and/or remnants of high elevated surfaces in
270 river long profiles. To highlight this dynamic evolution, we performed a morphometric analysis



271 of rivers all around the divide separating the Ebro basin from the Duero basin, with particular
272 attention given to the Aragonese branch of the Iberian Range (Fig. 4) and to the Rioja Trough
273 (Fig. 5) where captures have already been described.

274 The studied basins were digitally mapped using high-resolution (~30 meters) digital elevation
275 models (DEMs) from SRTM 1 Arc-Second Global elevation data available at the U.S.
276 Geological Survey (www.usgs.gov). The different DEMs were assembled using the ENVI
277 software. We also used 1:50,000 geological maps from the Instituto Geológico y Minero de
278 España (www.igme.es).

279 We used the TopoToolbox, a MATLAB-based software developed by Schwanghart and Scherler
280 (2014), to extract the river network and long profiles in our study area.

281

282 3.1 River capture evidences from geological, morphological and morphometric analyses

283

284 There are several evidences of recent river captures between the Ebro and Duero basins, as
285 previously described in the Jalon river and Bureba sectors (Gutiérrez-Santolalla et al., 1996;
286 Mikeš, 2010). This is also witnessed by the occurrence of high elevated surfaces at ~1000 m
287 a.s.l. delimited by major knickpoints in several river long profiles.

288

289 3.1.1 Jalon river area

290

291 The current Jalon river and its tributaries drain the Aragonese branch of the Iberian Range and
292 the eastern half of the Almazan subbasin, its western part belonging to the Duero catchment
293 (Fig. 4). Gutiérrez-Santolalla et al. (1996) pointed out several chronostratigraphic evidences
294 that allow to build a relative chronology of capture events in the Jalon network history. First,
295 the incision of the northern Paleozoic ridge and capture of the Calatayud basin by the Jalon
296 river is attributed to a post-Messinian age. The Jiloca river, the easternmost main Jalon tributary,
297 is then thought to capture the Daroca graben area to the east during the Late Pliocene – Early
298 Pleistocene. This is followed from the Early to Late Pleistocene by the capture of the Jiloca
299 graben to the southeast. As shown by our river long profile analyses, all these captures are
300 witnessed by knickpoints (Fig. 4). For instance, the capture of the Jiloca graben corresponds to
301 a major knickpoint in the Jiloca river profile that appears very smoothed, and that is followed
302 by an upstream ~50 km long flat domain preserved at ~1000 m high above sea level. This
303 imparts a convex shape to the Jiloca profile (Fig. 4). Due to the short period of time between
304 the formation of the Jiloca graben (the earliest glacial deposits are attributed to the Middle



305 Pliocene) and its capture (Early Pleistocene), we suggest this domain was a short-lived
306 endorheic domain that has never been drained before being captured by the Ebro network. In
307 the northwestern part of the Jiloca graben, the Cañamaria river, a tributary of the Jiloca river,
308 heads to the northwest, reaching the Gallocanta basin, also considered as a former graben
309 (Gracia, 1993b; Gracia et al., 1999; Gutiérrez-Elorza et al., 2002). The upstream part of its river
310 long profile is characterized by a sharper knickpoint at the entrance of the basin, and is followed
311 by a ~15 km long flat domain (Fig. 4). Similarly to the Jiloca graben, the Gallocanta basin
312 appears to be a short-lived endorheic domain that has been more recently captured by the Jiloca
313 river network.

314

315 According to Gutiérrez-Santolalla et al. (1996), the Jalon river reached the southern Paleozoic
316 ridge of the Aragonese branch, to the southwest of the Calatayud basin, captured the Munébrega
317 graben and the Almazan subbasin (also characterized by a pronounced knickpoint) during the
318 Pleistocene-Holocene, slightly after the capture of the Jiloca graben by the Jiloca river. This is
319 coherent with morphological evidences as the major knickpoint related to the capture of the
320 Jiloca graben appears very smoothed, whereas knickpoints observed in the west are sharper
321 suggesting they are younger.

322 For instance, the Piedra river (Jalon tributary) long profile shows major sharp knickpoints and
323 two successive ~30 km long almost flat domains in the Almazan subbasin, at ~900-1000 m
324 above sea level (Fig. 4). In addition, the upper reach of the river long profiles of the Jalon river,
325 and of its tributary the Blanco river, are characterized by major sharp knickpoints, and by a ~15
326 km long flat domain at ~1000-1100 m above sea level, in the Mesozoic Castillan branch of the
327 Iberian Range (Fig. 4).

328

329 3.1.2 The Rioja trough area

330

331 The Bureba area consists in folded Middle Cretaceous to Early Miocene series, covered by
332 undeformed Middle Miocene to Holocene deposits (Fig. 5). The main structural feature is the
333 Bureba anticline, orientated E-W to the west and NE-SW to the east, cored by Albian strata and
334 topped by Santonian limestones and dolomites. The western part of the anticline forms a
335 topographic ridge that controls the current location of the main drainage divide between the
336 Ebro and Duero river networks (Fig. 5). This ridge is incised by four rivers that are from west
337 to east, the Ubierna with the Jordan river, the Hoz, the Rioseras, and the Nava Solo rivers (Figs.
338 5, 7). Further east, the Diablo river does not incise the ridge and its headwater is located in the



339 core of the eastern branch of the Bureba anticline, the Fuente Valley (Fig. 5). The five last
340 streams are tributaries of the Ubierna river, which is a tributary of the Arlanzon river and so, of
341 the Duero river. To the north, the Ebro river system is represented, from west to east, by the
342 Homino river (a tributary of the Oca river) and its four tributaries, the Molina, the Fuente Monte,
343 the Zorica, and the San Pedro rivers (Figs. 5, 7). All these streams are outlined by Late
344 Pleistocene to Holocene alluvial series that are deposited at the bottom of their respective
345 valleys. Valleys from the Duero side appears larger than those from the Ebro side, which are
346 significantly more incised.

347 The Jordan river's headwater is located north of the ridge. We can continuously follow its valley
348 deposits northward along a broadly gentle slope, up to the locality of Coraegula (Fig. 5).
349 However, the current course of the Jordan river is cut ~8 km south, in the vicinity of Hontomin,
350 by the Homino (Ebro) river (Figs. 5B, C, 7). This fluvial capture is characterized by a well-
351 defined and highly incised elbow of capture and its river long profile shows a sharp knickpoint
352 located on Hontomin. Finally, there is a small wind gap on the divide between the two opposite
353 rivers (Figs. 5, 7).

354 To the southeast, the headwater of the Hoz river is located on the second ridge incision.
355 However, such incision is unlikely to result from the action of this headwater only as it would
356 necessitate more important water and sediment discharges, and so a larger drainage area
357 upstream. To the north, in the exact prolongation of the Hoz river, the Molina river shows a
358 remarkable bend similar to the elbow of capture previously described for the Homino river (Fig.
359 7). There is a minor knickpoint located on this elbow, according to the extracted river long
360 profile and such a ridge incision represents a well-defined wind gap between the two opposite
361 rivers (Figs. 5, 7, 8). Thus, it is likely that the Molina river used to represent the upper reach of
362 the Hoz river, before being captured by the Ebro network.

363 To the east, the Rioseras and the Nava Solo rivers have their headwater located on the third and
364 fourth ridge incision, respectively, also representing pronounced wind gaps. Similarly, in their
365 exact prolongations, the Fuente Monte and the Zorica rivers show important elbows of capture
366 with minor knickpoints. They may also represent former upper reaches of Duero streams that
367 have been captured by the Ebro network (Figs. 5, 7, 8).

368 Further east, the headwater of the Diablo river is located on the depression represented by the
369 core of the eastern branch of the Bureba anticline, the Fuente valley. In its prolongation to the
370 northeast, the San Pedro river incises the northeastern termination of the anticline from the
371 north before entering the valley, leading to a remarkable southward retreat of the divide (Fig.
372 5). Capture is again evidenced by important incision contrast between Ebro and Duero systems,



373 and by sharp knickpoints on the upper reach of the San Pedro river long profile when crossing
374 the Santonian dolomites (Fig. 8).

375

376 According to this whole set of observations, and in agreement with Mikeš (2010), we propose
377 that the western part of the Rioja trough has been recently captured by the Ebro drainage
378 network leading to a significant southwestward retreat of the main drainage divide, toward the
379 Duero basin (Fig. 7E).

380

381 3.1.3 Other capture features along the Ebro/Duero drainage divide

382

383 A similar capture pattern can be observed further west in the continuity of the Bureba anticline
384 (Fig. 5). The San Anton river shows a well-defined elbow of capture accompanied by a
385 smoothed knickpoint (See Fig. S1 in the Supplement) at its junction with the Rudron river (Ebro
386 tributary). The river course is highly incised toward the east, along the northern flank of the
387 WNW – ESE anticline, almost connecting to the upper reach of the Ubierna river. Valley
388 deposits are also observed in the continuity of the Ubierna valley, which former route is
389 witnessed by a wind gap (Fig. 5). However, this domain is no longer connected to its network
390 as it is now wandered from the North by the Nava river, a tributary of the Moradillo river, which
391 is a tributary of the Rudron river. This domain clearly recorded captures leading to divide
392 migration toward the Duero, in favor of the Ebro basin.

393

394 Both the Ebro river and several tributaries show high elevated ~10-20 km long flat domains at
395 ~800 – 1200 m a.s.l. and major knickpoints in the upper reach of their long profiles as the
396 Rudron, Queiles, and Alama rivers, as well as the Homino river and its tributaries: the Puerta
397 Nogales and Valdelanelala rivers (Figs. 5, 8; Fig. S1). All these domains may not be related to
398 surface uplift as they are not clearly associated to active tectonic features.

399 It has been shown that the occurrence of high elevated, low-relief surfaces, may result from
400 drainage reorganization leading to isolation and starvation of a drainage area, rather than
401 remnants of ancient erosional conditions or uplift (Yang et al., 2015). The Duero basin is
402 characterized by a high mean elevation (~1000 m) and by a very limited incision in the vicinity
403 of the Ebro/Duero drainage divide. A sudden divide migration toward the Duero basin is then
404 expected to isolate such high elevated and relatively preserved surfaces.



405 We suggest these flat domains have been recently captured by Ebro tributaries, and represent
406 remnants of Duero drainage areas, isolated due to important divide retreat toward the Duero
407 basin.

408 A lot of Ebro tributaries also show major knickpoints at ~1000 m a.s.l. close to the divide (Fig.
409 9; Fig. S1) that may also be linked with drainage divide migration. Overall, we consider a
410 paleodrainage divide delimited by these high-elevated knickpoints and flat domains, except for
411 the Jiloca graben area to the southeast, characterized by the occurrence of short-lived endorheic
412 domains (Fig. 9).

413

414 3.2 Chi (X) map

415 3.2.1 Background

416

417 The shape of the longitudinal profile of a river is classically described by a power law which
418 relates the local slope of the river to its drainage area (Flint, 1974):

419

$$420 \quad \frac{dz}{dx} = k_s A^{-\theta} \quad (1)$$

421

422 with z the elevation, x the distance, k_s a constant termed the channel steepness index, A the
423 drainage area and θ a constant termed the concavity index. In fluvial systems, the erosion rate
424 E is often expressed as a stream power erosion law (Whipple and Tucker, 1999):

425

$$426 \quad \frac{dz}{dt} = K A^m \left(\frac{dz}{dx} \right)^n \quad (2)$$

427

428 where t is the time, K is an erodibility coefficient, and m and n are constants. Under the
429 assumption of a steady-state between erosion (E) and uplift (U), that is $U = E = K A^m \left(\frac{dz}{dx} \right)^n$,
430 the expression of the stream power law can be rearranged to predict the steady-state shape of a
431 longitudinal profile of a river under constant climatic and tectonic forcing conditions:

432

$$433 \quad \frac{dz}{dx} = \left(\frac{U}{K} \right)^{\frac{1}{n}} A^{-\frac{m}{n}} \quad (3)$$

434



435 The comparison between equations (1) and (3) show that k_s may vary according to the uplift
436 rate and by consequent spatial variations in k_s can potentially be used to infer spatial variations
437 in U (Kirby and Whipple, 2012). In a region where spatial variations in U are not expected,
438 variations in k_s may also reflect disequilibrium along the river, on the form of a knickpoint for
439 example (Whipple and Tucker, 1999). Although the slope-area analysis of channel profiles is
440 potentially a powerful tool to evidence differences in the equilibrium state of rivers across
441 divide, and then to infer their migration (Willett et al., 2014), this method is limited and even
442 biased by the quality of the topographic data. Indeed, both a low-resolution of the DEM and
443 corrections brought to the DEM (filling or carving), lead to substantial uncertainties that are
444 automatically transferred to the slope, k_s and θ data. To avoid slope measurements, Royden et
445 al. (2000) proposed a procedure based on a coordinate transformation allowing linearizing river
446 profiles by using the elevation of each point along the profile (x) instead of the slope in the
447 stream power equation.

448 Considering steady-state with constant uplift rate and erodibility in time and space, Equation
449 (3) may be solved as follows:

450

$$451 \quad z(x) = z_b(x_b) + \frac{U}{KA_0^m} \frac{1}{n} X \quad (4)$$

452

453 where z_b is the elevation at the river's base level, A_0 is a reference scaling drainage area, and
454 χ is an integral function of the drainage area along the channel network.

455

$$456 \quad X = \int_{x_b}^x \left(\frac{A_0}{A(x)} \right)^{\frac{m}{n}} dx \quad (5)$$

457

458 A « X plot » (elevation versus X diagram) of a steady-state channel is then shown as a straight
459 line (Perron and Royden, 2013; Royden and Perron, 2013). This implies that channels pulled
460 away from this line are in disequilibrium and are expected to attempt to reach equilibrium.
461 Mapping χ on several watersheds and comparing χ across drainage divides is then a
462 potential way to elucidate the basins dynamics and reorganizations through captures (Willett et
463 al., 2014).

464 We used the Chi Analysis Tool developed by Mudd et al. (2014) to select the best m/n ratio and
465 to calculate χ throughout the connection between the Ebro and Duero basins from a similar
466 base level at 850 m a.s.l.



467

468 The best mean m/n ratio for all our streams is 0.425, which falls in the typical range (~0.4 –
469 0.6) characteristic of simple settings with uniform substrate, uplift rate and climate (Kirby and
470 Whipple, 2001, 2012; Wobus et al., 2006). The resulting map (Fig. 10) shows X values
471 calculated on different opposite streams in the vicinity of the Ebro/Duero drainage divide.
472 Similar values on both sides of the divide suggest the two opposite streams are at equilibrium,
473 whereas strong contrasted X values imply disequilibrium leading to divide migration,
474 continuously or through fluvial capture, toward the high values stream (Willett et al., 2014).

475

476 3.2.2 Application to the divide between the Ebro and Duero basins

477

478 The map of X values actually shows significant contrasting values across the Ebro/Duero divide.
479 We comment here these contrasts along the divide from the SE to the NW of the area considered
480 (Fig. 10).

481 There is a strong contrast in X values between the headwater of the Jalon river (Fig. 10),
482 characterized by low values (~300 m), and the closest part from the divide of the Bordecorex
483 river (Fig. 4), a tributary of the Duero river (~500 m). Such a disequilibrium implies divide
484 migration toward the Duero basin, predicting the capture of the uppermost reach of the
485 Bordecorex river by the Jalon river. To the north, tributaries of the Jalon river show slightly
486 lower X values than the tributaries of the Duero river. This suggests a relative equilibrium
487 although little captures may occur toward the Duero basin. A higher contrast is observed around
488 the easternmost part of the Duero basin, which is surrounded by the Ebro basin. The Araviana
489 river (tributary of the Duero river) seems to be taken in a bottleneck between the Manubles river
490 to the south and the Queiles river to the north (Fig. 4), which both show lower X values (Fig.
491 10). Toward the east, there is a strongest X values contrast between headwaters of the Araviana
492 river (>700 m) and of the Isuela (Jalon tributary) and Huecha rivers (<100 m). This domain
493 appears clearly in disequilibrium and is expected to be captured by the Ebro drainage network.
494 Such high X values differences appear also to the northwest (Fig. 10), in the southern part of
495 the Cameros basin where the Duero river and its tributaries' headwaters show X values >500-
496 700 m, whereas the facing rivers (Alama, Cidacos, Iregua, and Najerilla) are all characterized
497 by low X values <100 m. This predicts important disequilibrium and divide migration and
498 fluvial captures toward the south. Northwestward, X values between Duero and Ebro network
499 are more similar indicating that the divide is relatively more stable, up to the westernmost part
500 of the Ebro basin (Fig. 10). However, there are some slight localized X values contrasts (~200



501 / ~450 m) as observed between the Tiron and the Arlanzon rivers, between the Rudron and the
502 Ubierna and Urbel rivers, and between the Ebro and the Pisuerga rivers (Fig. 10). These suggest
503 minor local captures toward the Duero basin.

504

505 To sum up, X values calculated in the vicinity of the drainage divide between the Ebro and
506 Duero river networks show a general disequilibrium (Fig. 10) as the Ebro network is
507 characterized by low X values (up to ~200-300 m) compared to those for the Duero network
508 (up to ~450-700 m). In complement with all the evidences of divide displacements described
509 previously this allows predicting a general divide migration toward the Duero basin through
510 headwater retreat and river captures, in favor of the Ebro tributaries, especially around the
511 Almazan subbasin, which is expected to be entirely captured by the Ebro basin.

512

513 **4. Discussion**

514

515 4.1 A long term trend of divide migration

516

517 The oldest capture evidence in our study area corresponds to the incision of the northern part
518 of the Iberian Range by the Jalon river and by the capture of the Calatayud basin, attributed to
519 the post-Messinian (Gutiérrez-Santolalla et al. 1996). We show, by using morphological
520 evidences (Fig. 4) and in agreement with stratigraphic data, that the Jalon river system then
521 captured the Jiloca graben to the east since the Early Pleistocene, before progressively capturing
522 the Almazan subbasin toward the west, up to the Holocene (Gutiérrez-Santolalla et al. 1996).
523 From X analysis (Fig. 10), we deduced that the eastern part of the Duero basin, the Almazan
524 subbasin, is being actively captured by Ebro tributaries that drained the Iberian Range and the
525 Cameros basin. Despite low contrasts in X values, local captures are also evidenced in the
526 vicinity of the Ebro / Duero drainage divide toward the northwest. Capture is also well
527 witnessed by the occurrence of numerous high elevated (~1000 m) knickpoints and low-relief
528 surfaces (Figs. 5, 8, 9, 10).

529 Thus, there is a good correlation between X predictions and morphological and stratigraphic
530 data implying for a long continuity for capture and divide migration in favor of the Ebro basin
531 during Pliocene, Pleistocene, and Holocene times.

532

533 The pursuit of such a long capture trend can be driven by tectonic and/or climatic forcing
534 (Willett, 1999; Montgomery et al., 2001; Sobel et al., 2003; Sobel and Strecker, 2003; Bonnet,



535 2009; Whipple, 2009; Castelltort et al., 2012; Kirby and Whipple, 2012; Goren et al., 2015; Van
536 der Beek et al., 2016). However, such long-term trend of drainage reorganization may also
537 occur in tectonically quiescent domains, independently of such external forcing (Prince et al.,
538 2011). Here, the Iberian Range and the Cameros basin recorded extension pulses from the Late
539 Miocene to the Early Pleistocene, responsible for the formation of several grabens as previously
540 described (Gutiérrez-Santolalla et al., 1996; Capote et al., 2002). Extension events are also
541 recorded during the Holocene, nevertheless, the youngest erosion surface of Late Pliocene-
542 Early Pleistocene age observed in our study area shows no tectonic-related deformation and
543 reworking, suggesting that tectonic activity is reduced here (Gutiérrez-Elorza and Gracia,
544 1997). This is also consistent with the relative scarcity of seismic activity observed in our study
545 area, compared, for instance, to the Pyrenees, or to the Betics (Herraiz et al., 2000; Lacan and
546 Ortuño, 2012). We consequently propose that local tectonic activity is not the main driver to the
547 capture histories documented here, as most capture events postdate the cessation of tectonic
548 activity, and occur during intermediate quiescence episodes (Gutiérrez-Santolalla et al., 1996).

549

550 Although the Cameros basin shows relatively high mean annual precipitations up to ~1000
551 mm/an (Fig. 6) that are correlated with relatively high elevation (~1400-2200 m), the Ebro and
552 Duero basins show very similar and low values of ~400-500 mm/an (Hijmans et al., 2005), due
553 to global subarid climatic conditions. The Cameros area is the only place where a contrast in
554 precipitation pattern (Fig. 6) could potentially drive the migration of the divide toward the drier,
555 Duero area. Given that the same pattern is observed everywhere, even where there isn't any
556 precipitation difference, we suggest however that the present day climatic condition is unlikely
557 to control the general pattern of current drainage reorganization between the Ebro and Duero
558 basins. During the Pliocene and the Pleistocene, the climatic record in the northern Iberia
559 Peninsula is characterized by alternance between similar subarid conditions and intense
560 glaciation. However, there is no clear evidence of important glaciers development and related
561 erosion in our study area, especially for the Cameros basin and the Iberian Range (Ortigosa,
562 1994; García-Ruiz et al., 1998, 2016; Pellicer and Echeverría, 2004). This indicates that
563 drainage evolution between the Ebro and Duero basins is not clearly related to climatic
564 evolution.

565

566

567 4.2 Excavation of the Ebro basin as the main factor controlling drainage reorganization,
568 drainage divide migration and limiting incision of the Duero river



569

570 A striking morphological feature for river capture in our study area is that it is associated to an
571 important contrast in incision (e.g. Fig. 1B) from one side of the divide to the other, in
572 association with frequent knickpoints in the capturing reach (Fig. 9). This suggests that the
573 incision capacity of the river network is the main driver for capture and divide migration in our
574 setting. Then, to first order, both tectonic and climatic forcing does not appear to control
575 drainage reorganization between the Ebro and Duero basins.

576

577 The opening of the Ebro basin toward the Mediterranean Sea during the Late Miocene led to
578 important unfilling and widespread excavation (Garcia-Castellanos et al., 2003, Garcia-
579 Castellanos and Larrasoña, 2015), also favored by more humid and seasonal climatic
580 conditions (Calvo et al., 1993; Alonso-Zarza and Calvo, 2000). By contrast, incision related to
581 the opening of the Duero basin toward the Atlantic Ocean is concentrated to the west in the
582 Iberian Massif, characterized by a largescale knickzone (150 km long and 500 m high) in the
583 Duero river long profile (Fig. 1B), whereas propagation of incision eastward in the Cenozoic
584 part of the basin is limited (Antón et al., 2012, 2014), despite similar climatic conditions than
585 for the Ebro basin. An explanation resides in the fact that the resistant Iberian Massif basement
586 rocks may have controlled and limited incision and drainage reorganization in the Cenozoic
587 Duero basin (Antón et al., 2012). Then, the Duero profile upstream of this major knickzone
588 may be considered as a high elevated base level for its tributaries there. This contrast between
589 the Ebro and Duero base-levels implies a major contrast in fluvial dynamics, especially
590 regarding incision rate. We suggest the systematic and long-term trend of divide migration
591 toward the Duero basin and fluvial capture in favor of the Ebro basin since the Early Pliocene
592 is driven by this different incision behavior and from the widespread excavation resulting from
593 the opening of the Ebro basin toward the Mediterranean Sea since the Late Miocene.

594

595 The opening of the Ebro basin toward the Mediterranean Sea resulted in a drastic base level
596 down drop. We suggest this results in the establishment of an upstream-migrating incision wave
597 that propagates to every tributary of the Duero network, responsible for knickpoints migration
598 (Schumm et al., 1987; Whipple and Tucker, 1999; Yanites et al., 2013) and for drainage
599 reorganization and divide migration. The Chi analysis that we performed along the current
600 Ebro-Duero divide (Fig. 10) highlights areas where geomorphic disequilibrium still stands
601 today, which suggests that they are areas where divide is still mobile. The modelling study
602 performed by Garcia-Castellanos and Larrasoña (2015) suggests that the re-opening of the



603 Ebro basin occurred between 12.0 and 7.5 Ma. This indicates that the growth of the drainage
604 network of the Ebro basin and the establishment of new steady-state conditions is a long-lived
605 phenomenon, which is still not achieved today.

606

607 Incision in the Ebro basin leads to the capture of new drainage areas, whereas the Duero basin
608 recorded important loss of its own surface. The present day drained area of the Cenozoic Duero
609 basin, upstream of the major knickzone observed to the west in the Iberian Massif is ~63000
610 km². We described several domains along the Ebro-Duero divide that have clearly been recently
611 captured by the Ebro drainage network as the eastern part of the Almazan subbasin. In Figure
612 9, we have connected all these domains to define a « recent » captured area that used to belong
613 to the Duero basin. This area represents ~7700 km², which corresponds to ~12% of the present-
614 day Cenozoic Duero basin drainage area. Moreover, some of these captured domains record
615 relatively high precipitation rates as in the Cameros basin compared to the center of the Duero
616 basin. Such a reduction of the drainage area could have strong implications on the evolution of
617 the Duero basin, as important lowering of water and sediment fluxes, and so of incision
618 throughout the basin.

619 To better resolve the impact of such drainage area reduction on incision capacity, we perform a
620 stream power analysis of the Duero river. We consider the specific stream power, ω , defined as
621 $\omega = \rho g Q S / W$, where ρ is water density, g is gravitational acceleration, Q is discharge, S is
622 local river gradient, and W is river width (see the Supplement for details of the calculation).

623 We calculate ω for the present-day Duero river, and for a restored ancient Duero river that
624 drained this 12% of lost area. We plot the difference (ancient – present day) between the two
625 curves in Figure 11, with the Duero river long profile. Calculated difference in specific stream
626 power values are relatively low ($< 2 \text{ W m}^{-2}$) for the upstream part of the basin, but increase to
627 $\sim 5 \text{ W m}^{-2}$ when approaching the major knickzone at a distance of $\sim 350 \text{ km}$ from the river mouth.

628 The knickzone is characterized by peak values exceeding 10 W m^{-2} , which rapidly decrease to
629 $\sim 0 \text{ W m}^{-2}$ at the base of the knickzone ($\sim 200 \text{ km}$) and up to the river mouth (Fig. 11). Some
630 alternating peak and null values are observed in the lower reach of the river and may be related
631 to the occurrence of numerous dams along the river.

632 Overall, the specific stream power calculated for the ancient Duero river show higher values
633 than for the present day from the base of the knickzone to the uppermost reach of the river (Fig.
634 11). This implies a general decrease of the Duero river's incision capacity between this ancient
635 state to the present day. The remarkable difference of stream power values in the vicinity of the
636 knickzone (Fig. 11) suggests that drainage area reduction limits erosion in the Duero basin as it



637 helps for preservation of the lithologic barrier to the west, considered as an intermediate base
638 level (Antón et al., 2012).

639

640 This stream power calculation does not take into account possible captures and divide migration
641 in other areas around the Duero basin, nor the full history of the divide migration through time.
642 Some contrasts of incision are also observed in the Central Range to the South, and in the
643 Cantabrian domain to the North. Both show more important incision than in the Duero basin
644 suggesting potential river captures and divide migration at the expense of the Duero basin,
645 increasing the total of lost drainage area, especially in domains where precipitation rates are
646 higher than inside the basin (Fig. 6).

647 We then suggest that the area loss for the Duero basin partly due to important capture and
648 incision in the Ebro basin is responsible for an important decrease of the incision capacity in
649 the Duero basin. Then, active exorheism in the Ebro basin is likely responsible for the present
650 day quasi-endorheic state of the Duero basin.

651

652

653 Conclusions

654

655 The Ebro and Duero basins both recorded a long endorheic stage during Oligocene and Miocene
656 times. Since the Late Miocene, the Ebro basin is opened to the Mediterranean Sea and record
657 important unfilling. This results in important incision driven by a very active drainage network.
658 By contrast, the Duero basin is opened to the Atlantic Ocean since the Late Miocene – Early
659 Pliocene and record only limited incision. Its upper part is considered as still almost endorheic.
660 Such contrast in river-driven incision leads to important drainage reorganization between the
661 two basins as shown by numerous occurrences of river captures by the Ebro basin network, and
662 divide migration toward the Duero basin. Drainage area lost results then in the lowering of the
663 incision capacity of the Duero basin favoring its almost endorheic stage.

664

665

666 Author contributions

667 AV undertook morphometric modeling and interpretation, and wrote the paper. SB and FM
668 contributed to the interpretation and the writing.

669

670



671 Competing interests.

672 The authors declare that they have no conflict of interest.

673

674 Acknowledgements.

675 This study was funded by the OROGEN Project, a TOTAL-BRGM-CNRS consortium.

676

677

678 References

679

680 Alonso-Zarza, A. M. and Calvo, J. P.: Palustrine sedimentation in an episodically subsiding
681 basin: the Miocene of the northern Teruel Graben (Spain), *Palaeogeo., Palaeoclimatol.,*
682 *Palaeoecol.*, 160, 1-21, 2000.

683

684 Alonso-Zarza, A. M., Armenteros, I., Braga, J. C., Muñoz, A., Pujalte, V., Ramos, E., Aguirre,
685 J., Alonso-Gavilán, G., Arenas, C., Ignacio Baceta, J., Carballeira, J., Calvo, J. P., Corrochano,
686 A., Fornós, J. J., González, A., Luzón, A., Martín, J. M., Pardo, G., Payros, A., Pérez, A., Pomar,
687 L., Rodriguez, J. M., and Villena, J.: Tertiary, in: *The Geology of Spain*, Gibbons, W. and
688 Moreno, T. (Eds.): The Geological Society, London, 293-334, 2002.

689

690 Antón, L., Rodés, A., De Vicente, G., Pallàs, R., Garcia-Castellanos, D., Stuart, F. M., Braucher,
691 R., and Bournès, D.: Quantification of fluvial incision in the Duero Basin (NW Iberia) from
692 longitudinal profile analysis and terrestrial cosmogenic nuclide concentrations, *Geomorph.*,
693 165-166, 50-61, <https://doi.org/10.1016/j.geomorph.2011.12.036>, 2012.

694

695 Antón, L., Rodés, A., De Vicente, G., and Stokes, M.: Using river long profiles and geomorphic
696 indices to evaluate the geomorphological signature of continental scale drainage capture, Duero
697 basin (NW Iberia), *Geomorph.*, 206, 250-261, <https://doi.org/10.1016/j.geomorph.2013.09.028>,
698 2014.

699

700 Babault, J., Loget, N., Van Den Driessche, J., Castelltort, S., Bonnet, S., and Davy, P.: Did the
701 Ebro basin connect to the Mediterranean before the Messinian salinity crisis ?, *Geomorph.*, 81,
702 155-165, <https://doi.org/10.1016/j.geomorph.2006.04.004>.

703



- 704 Barrón, E., Postigo-Mijarra, J. M., and Casas-Gallego, M.: Late Miocene vegetation and climate
705 of the La Cerdanya Basin (eastern Pyrenees, Spain), *Rev. Palaeobot. Palynol.*, 235, 99-119,
706 <https://doi.org/10.1016/j.revpalbo.2016.08.007>, 2016.
707
- 708 Bartolomé, M., Sancho, C., Moreno, A., Oliva-Urcia, B., Belmonte, Á., Bastida, J., Cheng, H.,
709 and Edwards, R. L.: Upper Pleistocene interstratal piping-cave speleogenesis: The Seso Cave
710 System (Central Pyrenees, Northern Spain), *Geomorph.*, 228, 335-344,
711 <https://doi.org/10.1016/j.geomorph.2014.09.007>, 2015.
712
- 713 Bessais, E. and Cravatte, J.: Les écosystèmes végétaux Pliocènes de Catalogne Méridionale.
714 Variations latitudinales dans le domaine Nord-Ouest Méditerranéen, *Geobios*, 21, 49-63, 1988.
715
- 716 Bond, J.: Tectono-sedimentary evolution of the Almazan Basin, NE Spain, in: Friend, F. and
717 Dabrio, C. (Eds.): Tertiary Basins of Spain: the Stratigraphic Record of Crustal Kinematics,
718 World and Regional Geology, 6, Cambridge University Press, Cambridge, 203-213, 1996.
719
- 720 Bonnet, S.: Shrinking and splitting of drainage basins in orogenic landscapes from the migration
721 of the main drainage divide, *Nat. Geosc.*, 90, 766-771, <https://doi.org/10.1038/NGEO666>,
722 2009.
723
- 724 Brocklehurst, S. H. and Whipple, K. X.: Glacial erosion and relief production in the Eastern
725 Sierra Nevada, California, *Geomorph.*, 42, 1-24, 2002.
726
- 727 Calvo, J. P., Daams, R., and Morales, J.: Up-to-date Spanish continental Neogene synthesis and
728 paleoclimatic interpretation. *Revista de la Sociedad Geologica de España*, 6, 29-40, 1993.
729
- 730 Capote, R., Muñoz, J. A., Simón, J. L., Liesa, C. L., and Arlegui, L. E.: Alpine tectonics 1: the
731 Alpine system north of the Betic Cordillera, in: The Geology of Spain, Gibbons, W. and
732 Moreno, T. (Eds.): The Geological Society, London, 367-400, 2002.
733
- 734 Castelltort, S., Goren, L., Willett, S. D., Champagnac, J. D., Herman, F., and Braun, J.: River
735 drainage patterns in the New Zealand Alps primarily controlled by plate tectonic strain. *Nat.*
736 *Geosci.*, 5, 744-748, <https://doi.org/10.1038/ngeo1582>, 2012.
737



- 738 Colomer i Busquets, M., and Santanach i Prat, P.: Estructura y evolucion del borde sur-
739 occidental de la Fosa de Calatayud-Daroca, *Geogaceta*, 4, 29-31, 1988.
- 740
- 741 Coney, P. J., Muñoz, J. A., McClay, K. R., and Evenchick, C. A.: Syntectonic burial and post-
742 tectonic exhumation of the southern Pyrenees foreland fold-thrust belt, *J. Geol. Soc. London*,
743 153, 9-16, <https://doi.org/10.1144/gsjgs.153.1.0009>, 1996.
- 744
- 745 Costa, E., Garcés, M., López-Blanco, M., Beamud, E., Gómez-Paccard, M., and Larrasoña, J.
746 C.: Closing and continentalization of the South Pyrenean foreland basin (NE Spain):
747 magnetochronological constraints, *Basin Res.*, 22, 904-917, [https://doi.org/10.1111/j.1365-](https://doi.org/10.1111/j.1365-2117.2009.00452.x)
748 2117.2009.00452.x, 2010.
- 749
- 750 Delmas, M., Calvet, M., and Gunnell, Y.: Variability of Quaternary glacial erosion rates – A
751 global perspective with special reference to the Eastern Pyrenees, *Quat. Sci. Rev.*, 28, 484-498,
752 <https://doi.org/10.1016/j.quascirev.2008.11.006>, 2009.
- 753
- 754 Del Rio, P., Barbero, L., and Stuart, F. M.: Exhumation of the Sierra de Cameros (Iberian Range,
755 Spain): constraints from low-temperature thermochronologie, in: Liesker, F., Ventura, B., and
756 Glasmacher, U. A. (Eds.): *Thermochronological Methods: From Palaeotemperature Constraints*
757 *to Landscape Evolution Models*, Geological Society, London, Special Publications, 324, 154-
758 166, <https://doi.org/10.1144/SP324.12>, 2009.
- 759
- 760 De Vicente, G., Vegas, R., Muñoz, M. A., Silva, P. G., Andriessen, P., Cloetingh, S., González-
761 Casado, J. M., Van Wees, J. D., Álvarez, J., Carbó, A., and Olaiz, A.: Cenozoic thick-skinned
762 deformation and topography evolution of the Spanish Central System, *Glob. Planet. Change*,
763 58, 335-381, <https://doi.org/10.1016/j.gloplacha.2006.11.042>, 2007.
- 764
- 765 Duval, M., Sancho, C., Calle, M., Guilarte, V., and Peña-Monné, J. L.: On the interest of using
766 the multiple center approach in ESR dating of optically bleached quartz grains: Some examples
767 from the Early Pleistocene terraces of the Alcanadre River (Ebro basin, Spain), *Quat.*
768 *Geochronol.*, 29, 58-69, <https://doi.org/10.1016/j.quageo.2015.06.006>, 2015.
- 769



- 770 Fillon, C. and Van der Beek, P.: Post-orogenic evolution of the southern Pyrenees: constraints
771 from inverse thermo-kinematic modelling of low-temperature thermochronology data, *Basin*
772 *Res.*, 23, 1-19, <https://doi.org/10.1111/j.1365-2117.2011.00533.x>, 2012.
773
- 774 Fillon, C., Gautheron, C., and Van der Beek, P.: Oligocene-Miocene burial and exhumation of
775 the Southern Pyrenean foreland quantified by low-temperature thermochronology, *J. Geol. Soc.*
776 *London*, 170, 67-77, <https://doi.org/10.1144/jgs2012-051>, 2013.
777
- 778 Flint, J.J.: Stream gradient as a function of order, magnitude, and discharge, *Water Resources*
779 *Res.*, 10, 969-973, 1974.
780
- 781 Garcia-Castellanos, D.: Long-term evolution of tectonic lakes: Climatic controls on the
782 development of internally drained basins, *Geol. Soc. Am., Spec. Paper*, 398, 283-294,
783 [https://doi.org/10.1130/2006.2398\(17\)](https://doi.org/10.1130/2006.2398(17)), 2006.
784
- 785 Garcia-Castellanos, D. and Larrasoana, J. C.: Quantifying the post-tectonic topographic
786 evolution of closed basins: The Ebro basin (northeast Iberia), *Geology*, 43, 663-666,
787 <https://doi.org/10.1130/G36673.1>, 2015.
788
- 789 Garcia-Castellanos, D., Vergés, J., Gaspar-Escribano, J., and Cloething, S.: Interplay between
790 tectonics, climate, and fluvial transport during the Cenozoic evolution of the Ebro Basin (NE
791 Iberia), *J. Geophys. Res.*, 108, 2347, <https://doi.org/10.1029/2002JB002073>, 2003.
792
- 793 García-Ruiz, J. M., Ortigosa, L. M., Pellicer, F., and Arnáez, J.: Geomorfología glaciar del
794 Sistema Ibérico, in: Gómez-Ortiz, A. and Pérez-Alberti, A. (Eds.): *Las huellas glaciares de las*
795 *montañas españolas*, Universidad de Santiago de Compostela, 347-381, 1998.
796
- 797 García-Ruiz, J. M., Palacios, D., González-Sampériz, P., De Andrés, N., Moreno, A., Valero-
798 Garcés, B., and Gómez-Villar, A.: Mountain glacier evolution in the Iberian Peninsula during
799 the Younger Dryas, *Quat. Sci. Rev.*, 138, 16-30,
800 <https://doi.org/10.1016/j.quascirev.2016.02.022>, 2016.
801



- 802 Goren, L., Castelltort, S., and Klinger, Y.: Modes and rates of horizontal deformation from
803 rotated river basins: Application to the Dead Sea fault system in Lebanon, *Geology*, 43, 843-
804 846, <https://doi.org/10.1130/G36841.1>, 2015.
- 805
- 806 Gracia, F. J.: Tectonica pliocena de la Fosa de Daroca (prov. De Zaragoza), *Geogaceta*, 11, 127-
807 129, 1992.
- 808
- 809 Gracia, F. J.: Evolucion cuaternaria del rio Jiloca (Cordillera Iberica Central), in: Fumanal, M.
810 P. and Bernabeu, J. (Eds.): *Estudios sobre Cuaternario, Medios Sedimentarios, Cambios*
811 *Ambientales, Habitat Humano*, Valencia, 43-51, 1993a.
- 812
- 813 Gracia, F. J.: Evolucion geomorfologica de la region de Gallocanta (Cordillera Iberica Central),
814 *Geographicalia*, 30, 3-17, 1993b.
- 815
- 816 Gracia, F. J., Gutiérrez-Santolalla, F., and Gutiérrez-Elorza, M.: Evolucion geomorfologica del
817 polje de Gallocanta (Cordillera Ibérica), *Revista Sociedad Geologica de España*, 12, 351-368,
818 1999.
- 819
- 820 Gracia, F. J. and Cuchi, J. A.: Control tectonico de los travertinos fluviales del rio Jiloca
821 (Cordillera Ibérica), in: *El Cuaternario en España y Portugal, Actas 2a Reun. Cuat. Ibérico,*
822 *AEQUA y CTPEQ*, Madrid-1989, 2, 697-706, 1993.
- 823
- 824 Guimerà, J., Mas, R., and Alonso, Á.: Intraplate deformation in the NW Iberian Chain:
825 Mesozoic extension and Tertiary contractional inversion, *J. Geol. Soc. London*, 161, 291-303,
826 <https://doi.org/10.1144/0016-764903-055>, 2004.
- 827
- 828 Gutiérrez-Elorza, M. and Gracia, F. J.: Environmental interpretation and evolution of the
829 Tertiary erosion surfaces in the Iberian Range (Spain), in: Widdowson, M. (Ed.):
830 *Palaeosurfaces: Recognition, Reconstruction and Palaeoenvironmental Interpretation,*
831 *Geological Society Special Publication*, 120, 147-158, 1997.
- 832
- 833 Gutiérrez-Elorza, M., García-Ruiz, J. M., Goy, J. L., Gracia, F. J., Gutiérrez-Santolalla, F.,
834 Martí, C., Martín-Serrano, A., Pérez-González, A., and Zazo, C.: Quaternary, in: *The Geology*
835 *of Spain*, Gibbons, W. and Moreno, T. (Eds.): *The Geological Society*, London, 335-366, 2002.



836

837 Gutiérrez-Santolalla, F., Gracia, F. J., and Gutiérrez-Elorza, M.: Consideraciones sobre el final
838 del relleno endorreico de las fossa de Calatayud y Teruel y su paso al exorreísmo. Implicaciones
839 morfoestratigráficas y estructurales, in : Grandal d'Ánglade, A. and Pagés-Valcarlos, J. (Eds.) :
840 IV Reunion de Geomorfología, Sociedad Española de Geomorfología, O Castro (A Coruña),
841 23-43, 1996.

842

843 Herraiz, M., De Vicente, G., Lindo-Ñaupari, R., Giner, J., Simón, J. L., González-Casado, J.
844 M., Vadillo, O., Rodríguez-Pascua, M. A., Cicuéndez, J. I., Casas, A., Cabañas, L., Rincón, P.,
845 Cortés, A. L., Ramírez, M., and Lucini, M.: *Tectonics*, 19, 762-786, 2000.

846

847 Hijmans, R. J., Cameron, S. E., Parra, J. L., Jones, P. G., and Jarvis, A.: Very high resolution
848 interpolated climate surfaces for global land areas, *Int. J. Climatol.*, 25, 1965-1978,
849 <https://doi.org/10.1002/joc.1276>, 2005.

850

851 Jiménez-Moreno, G., Fauquette, S., and Suc, J. P.: Miocene to Pliocene vegetation
852 reconstruction and climate estimates in the Iberian Peninsula from pollen data, *Rev. Palaeobot.*
853 *Palynol.*, 162, 403-415, <https://doi.org/10.1016/j.revpalbo.2009.08.001>, 2010.

854

855 Jiménez-Moreno, G., Burjachs, F., Expósito, I., Oms, O., Carrancho, Á., Villalaín, J. J., Agustí,
856 J., Campeny, G., Gómez de Soler, B., and Van der Made, J.: Late Pliocene vegetation and
857 orbital-scale climate changes from the western Mediterranean area, *Global Planet. Change*, 108,
858 15-28, <https://doi.org/10.1016/j.gloplacha.2013.05.012>, 2013.

859

860 Jurado, M. J. and Riba, O.: The Rioja area (westernmost Ebro basin): a ramp valley with
861 neighbouring piggybacks, in: Friend, P. and Dabrio, C. (Eds.): *Tertiary basins of Spain*, *World*
862 *and Regional Geology*, 6, Cambridge University Press, Cambridge, 173-179, 1996.

863

864 Kirby, E. and Whipple, K. X.: Quantifying differential rock uplift rates via stream profile
865 analysis, *Geology*, 29, 415-418, 2001.

866

867 Kirby, E. and Whipple, K. X.: Expression of active tectonics in erosional landscapes, *J. Struct.*
868 *Geol.*, 44, 54-75, <https://doi.org/10.1016/j.jsg.2012.07.009>, 2012.

869



- 870 Kuhlemann, J., Frisch, W., Dunkl, I., Székely, D., and Spiegel, C.: Miocene shifts of the
871 drainage divide in the Alps and their foreland basin, *Z. Geomorph.*, 45, 239-265, 2001.
872
- 873 Lacan, P. and Ortuño, M.: Active tectonics of the Pyrenees: a review, *J. Iberian Geol.*, 38, 9-30,
874 https://doi.org/10.5209/rev_JIGE.2012.v38.n1.39203, 2012.
875
- 876 Larrasoaña, J. C., Murelaga, X., and Garcés, M.: Magnetobiochronology of Lower Miocene
877 (Ramblian) continental sediments from the Tuleda Formation (western Ebro basin, Spain), *Ea.*
878 *Planet. Sci. Lett.*, 243, 409-423, <https://doi.org/10.1016/j.epsl.2006.01.034>, 2006.
879
- 880 López-Blanco, M., Marzo, M., Burbank, D. W., Vergés, J., Roca, E., Anadón, P., and Piña, J.:
881 Tectonic and climatic controls on the development of foreland fan deltas: Montserrat and Sant
882 Llorenç del Munt systems (Middle Eocene, Ebro Basin, NE Spain), *Sediment. Geol.*, 138, 17-
883 39, 2000.
884
- 885 López-Martínez, N., García-Moreno, E., and Álvarez-Sierra, A.: Paleontología y
886 bioestratigrafía (micromamíferos) del Mioceno medio y superior del sector central de la cuenca
887 del Duero, *Studia Geologica Salmanticensia*, Ediciones Universidad Salamanca, 22, 191-212,
888 1986.
889
- 890 Martín-Chivelet, J., Berástegui, X., Rosales, I., Vilas, L., Vera, J. A., Caus, E., Gräfe, K. U.,
891 Mas, R., Puig, C., Segura, M., Robles, S., Floquet, M., Quesada, S., Ruiz-Ortiz, P. A., Fregenal-
892 Martínez, M. A., Salas, R., Arias, C., García, A., Martín-Algarra, A., Meléndez, M. N., Chacón,
893 B., Molina, J. M., Sanz, J. L., Castro, J. M., García-Hernández, M., Carenas, B., García-
894 Hidalgo, J., Gil, J., and Ortega, F.: Cretaceous, in: *The Geology of Spain*, Gibbons, W. and
895 Moreno, T. (Eds.): The Geological Society, London, 255-292, 2002.
896
- 897 Martín-Serrano, A.: La definición y el encajamiento de la red fluvial actual sobre el macizo
898 hesperico en el marco de su geodinamica alpina, *Rev. Soc. Geol. España*, 4, 337-351, 1991.
899
- 900 Mikeš, D.: The Upper Cenozoic evolution of the Duero and Ebro fluvial systems (N-Spain):
901 Part 1. Paleogeography; Part 2. Geomorphology, *Cent. Eur. J. Geosci.*, 2, 320-332,
902 <https://doi.org/10.2478/v10085-010-0017-4>, 2010.
903



- 904 Montgomery, D. R., Balco, G., and Willett, S. D.: Climate, tectonics, and the morphology of
905 the Andes, *Geology*, 29, 579-582, 2001.
- 906
- 907 Moreno, D., Falguères, C., Pérez-González, A., Duval, M., Voinchet, P., Benito-Calvo, A.,
908 Ortega, A. I., Bahain, J. J., Sala, R., Carbonell, E., Bermúdez de Castro, J. M., and Arsuaga, J.
909 L.: ESR chronology of alluvial deposits in the Arlanzon valley (Atapuerca, Spain):
910 Contemporaneity with Atapuerca Gran Dolina site, *Quat. Geochronol.*, 10, 418-423,
911 <https://doi.org/10.1016/j.quageo.2012.04.018>, 2012.
- 912
- 913 Moreno, D., Belmonte, A., Bartolomé, M., Sancho, C., Oliva, C., Stoll, H., Edwards, L. R.,
914 Cheng, H., and Hellstrom, J.: Formacion de espeleotemas en el noreste peninsular y su relacion
915 con las condiciones climaticas durante los ultimos ciclos glaciares, *Cuadernos de Investigacion*
916 *Geografica*, 39, 25-47, 2013.
- 917
- 918 Mudd, S., Attal, M., Milodowski, D. T., Grieve, S. W. D., and Valters, D. A.: A statistical
919 framework to quantify spatial variation in channel gradients using the integral method of
920 channel profile analysis, *J. Geophys. Res.- Earth Surf.*, 119, 138-152,
921 <https://doi.org/10.1002/2013JF002981>, 2014.
- 922
- 923 Muñoz-Jiménez, A. and Casas-Sainz, A. M.: The Rioja Trough (N Spain): tectonosedimentary
924 evolution of a symmetric foreland basin, *Basin Res.*, 9, 65-85, 1997.
- 925
- 926 Nivière, B., Lacan, P., Regard, V., Delmas, M., Calvet, M., Huyghe, D., and Roddaz, B.:
927 Evolution of the Late Pleistocene Aspe River (Western Pyrenees, France). Signature of climatic
928 events and active tectonics, *Comptes Rendus Geosci.*, 348, 203-212, <https://doi.org/10.1016/j.crte.2015.07.003>, 2016.
- 929
- 930
- 931 Ortigosa, L. M.: Las grandes unidades des relieve, *Geografía de la Rioja*, 1, 62-71, 1994.
- 932
- 933 Palacios, D., Andrés, N., De Marcos, J., and Vásquez-Selem, L.: Maximum glacial advance and
934 deglaciation of the Pinar Valley (Sierra de Gredos, Central Spain) and its significance in the
935 Mediterranean context, *Geomorph.*, 177-178, 51-61,
936 <https://doi.org/10.1016/j.geomorph.2012.07.013>, 2012.
- 937



- 938 Palacios, D., De Marcos, J., and Vásquez-Selem, L.: Last Glacial Maximum and deglaciation
939 of the Sierra de Gredos, central Iberian Peninsula, *Quat. Int.*, 233, 16-26,
940 <https://doi.org/10.1016/j.quaint.2010.04.029>, 2011.
- 941
- 942 Pellicer, F. and Echeverría, M. T.: El modelado glaciar y periglaciar en el macizo del moncayo,
943 in: Peña, J. L., Longares, L. A., and Sánchez, M. (Eds.): *Geografía Física de Aragón, Aspectos*
944 *generals y tematicos*, Universidad de Zaragoza e Institucion Fernando el Catolico, Zaragoza,
945 173-185, 2004.
- 946
- 947 Pérez-Rivarés, F. J., Garcés, M., Arenas, C., and Pardo, G.: Magnetocronología de la sucesion
948 Miocena de la Sierra de Alcubierre (sector central de la cuenca del Ebro), *Rev. Soc. Geol.*
949 *España*, 15, 217-231, 2002.
- 950
- 951 Pérez-Rivarés, F. J., Garcés, M., Arenas, C., and Pardo, G.: Magnetostratigraphy of the Miocene
952 continental deposits of the Montes de Castejon (central Ebro basin, Spain): geochronological
953 and paleoenvironmental implications, *Geologica Acta*, 2, 221-234, 2004.
- 954
- 955 Perron, J. T. and Royden, L.: An integral approach to bedrock river profile analysis. *Earth Surf.*
956 *Process. Landforms*, 38, 570–576, <https://doi.org/10.1002/esp.3302>, 2013.
- 957
- 958 Prince, P. S., Spotila, J. A., and Henika, W. S.: Stream capture as driver of transient landscape
959 evolution in a tectonically quiescent setting, *Geology*, 39, 823–826,
960 <https://doi.org/10.1130/G32008.1>, 2011.
- 961
- 962 Puigdefàbregas, C., Muñoz, J. A., and Vergés, J.: Thrusting and foreland basin evolution in the
963 Southern Pyrenees, in: *Thrust Tectonics*, McClay, K.R. (Ed.): Chapman & Hall, London, 247-
964 254, 1992.
- 965
- 966 Pulgar, J. A., Alonso, J. L., Espina, R. G., and Marín, J. A.: La deformacion alpine en el
967 basamento varisco de la Zona Cantabrica, 283-294, 1999.
- 968
- 969 Riba, O., Reguant, S., and Villena, J.: Ensayo de sintesis estratigrafica y evolutiva de la Cuenca
970 terciaria del Ebro, in: Comba, J. A. (Ed.): *Geologia de España*, 2, Libro Jubila J. M. Rios,
971 Instituto Geologico y Minero de España, Madrid, 131-159.



- 972
- 973 Rivas-Carballo, M. R., Alonso-Gavilán, G., Valle, M. F., and Civis, J.: Miocene Palynology of
974 the central sector of the Duero Basin (Spain) in relation to palaeogeography and
975 palaeoenvironment, *Rev. Palaeobot. Palynol.*, 82, 251-264, 1994.
- 976
- 977 Royden, L. and Perron, J. T.: Solutions of the stream power equation and application to the
978 evolution of river longitudinal profiles, *J. Geophys. Res.- Earth Surf.*, 118, 497-518,
979 <https://doi.org/10.1002/jgrf.20031>, 2013.
- 980
- 981 Royden, L. H., Clark, K., and Whipple, K. X.: Evolution of river elevation profiles by bedrock
982 incision: analytical solutions for transient river profiles related to changing uplift and
983 precipitation rates, *EOS, Transactions of the American Geophysical Union* 81, Fall Meeting
984 Supplement, Abstract T62F-09, 2000.
- 985
- 986 Salas, R., Guimerà, J., Mas, R., Martín-Closas, C., Meléndez, A., and Alonso, A.: Evolution of
987 the Mesozoic Central Iberian Rift System and its Cainozoic inversion (Iberian Chain), in:
988 Ziegler, P. A., Cavazza, W., Robertson, A. F. H., and Crasquin-Soleau, S. (Eds.): Peri-Tethys
989 Memoir 6: Peri-Tethyan Rift/Wrench Basins and Passive Margins. *Mémoires du Muséum*
990 *national d'Histoire naturelle*, 186, 145-185, 2001.
- 991
- 992 Sancho, C., Calle, M., Peña-Monné, J. L., Duval, M., Oliva-Urcia, B., Pueyo, E. L., Benito, G.,
993 and Moreno, A.: Dating the Earliest Pleistocene alluvial terrace of the Alcanadre River (Ebro
994 Basin, NE Spain): Insights into the landscape evolution and involved processes, *Quat. Int.*, 407,
995 86-95, <https://doi.org/10.1016/j.quaint.2015.10.050>, 2016.
- 996
- 997 Schumm, S. A., Mosley, M. P., and Weaver, W. E.: *Experimental fluvial geomorphology*, John
998 Wiley and Sons, New York, pp. 413, 1987.
- 999
- 1000 Schwanghart, W. and Scherler, D.: TopoToolbox 2 a MATLAB-based software for topographic
1001 analysis and modeling in Earth surface sciences, *Earth Surf. Dynamics*, 2, 1-7,
1002 <https://doi.org/10.5194/esurf-2-1-2014>, 2014.
- 1003



- 1004 Serrano, E., González-Trueba, J. J., Pellitero, R., González-García, M., and Gómez-Lende, M.:
1005 Quaternary glacial evolution in the Central Cantabrian Mountains (Northern Spain),
1006 *Geomorph.*, 196, 65-82, <https://doi.org/10.1016/j.geomorph.2012.05.001>, 2013.
1007
- 1008 Serrano, E., González-Trueba, J. J., Pellitero, R., Gómez-Lende, M.: Quaternary glacial history
1009 of the Cantabrian Mountains of northern Spain: a new synthesis, in: Hughes, P. D. and
1010 Woodward, J. C. (Eds.): *Quaternary Glaciation in the Mediterranean Mountains*, Geological
1011 Society, London, Special Publications, 433, <https://doi.org/10.1144/SP433.8>, 2016.
1012
- 1013 Sobel, E. R. and Strecker, M. R.: Uplift, exhumation and precipitation: tectonic and climatic
1014 control of Late Cenozoic landscape evolution in the northern Sierras Pampeanas, Argentina,
1015 *Basin Res.*, 15, 431-451, <https://doi.org/10.1046/j.1365-2117.2003.00214.x>, 2003.
1016
- 1017 Sobel, E. R., Hilley, G. E., and Strecker, M. R.: Formation of internally drained contractional
1018 basins by aridity-limited bedrock incision, *J. Geophys. Res.*, 108, 2344,
1019 <https://doi.org/10.1029/2002JB001883>, 2003.
1020
- 1021 Stange, K. M., Van Balen, R. T., Garcia-Castellanos, D., and Cloething, S.: Numerical
1022 modelling of Quaternary terrace staircase formation in the Ebro foreland basin, southern
1023 Pyrenees, NE Iberia, *Basin Res.*, 1-23, <https://doi.org/10.1111/bre.12103>, 2014.
1024
- 1025 Suc, J. P. and Popescu, S. M.: Pollen records and climatic cycles in the Mediterranean region
1026 since 2.7 Ma, in: Head, M. J. and Gibbard, P. L. (Eds.): *Early-Middle Pleistocene Transitions,*
1027 *the Land-Ocean Evidence*, Geological Society, London, Special Publications, 247, 147-158,
1028 <https://doi.org/10.1144/GSL.SP.2005.247.01.08>, 2005.
1029
- 1030 Urgeles, R., Camerlenghi, A., Garcia-Castellanos, D., De Mol, B., Garcés, M., Vergés, J.,
1031 Haslam, I., and Hardman, M.: New constraints on the Messinian sealevel drawdown from 3D
1032 seismic data of the Ebro Margin, western Mediterranean, *Basin Res.*, 23, 123-145,
1033 <https://doi.org/10.1111/j.1365-2117.2010.00477.x>, 2010.
1034
- 1035 Van der Beek, P., Litty, C., Baudin, M., Mercier, J., Robert, X., and Hardwick, E.: Contrasting
1036 tectonically driven exhumation and incision patterns, western versus central Nepal Himalaya,
1037 *Geology*, 44, 327-330, <https://doi.org/10.1130/G37579.1>, 2016.



1038

1039 Vázquez-Urbez, M., Arenas, C., Pardo, G., and Pérez-Rivarés, J.: The effect of drainage
1040 reorganization and climate on the sedimentologic evolution of intermontane lake systems: the
1041 final fill stage of the Tertiary Ebro Basin (Spain), *J. Sediment. Res.*, 83, 562-590,
1042 <https://doi.org/10.2110/jsr.2013.47>, 2013.

1043

1044 Villena, J., Pardo, G., Pérez, A., Muñoz, A., and González, A.: The Tertiary of the Iberian margin
1045 of the Ebro basin: palaeogeography and tectonic control, in: Friend, P. and Dabrio, C. (Eds.):
1046 Tertiary basins of Spain, *World and Regional Geology*, 6, Cambridge University Press,
1047 Cambridge, 83-88, 1996.

1048

1049 Whipple, K.: The influence of climate on the tectonic evolution of mountain belts, *Nature*
1050 *Geosci.*, 2, 97-104, <https://doi.org/10.1038/ngeo638>, 2009.

1051

1052 Whipple, K. X. and Tucker, G. E.: Dynamics of the stream-power river incision model:
1053 Implications for height limits of mountain ranges, landscape response timescales, and research
1054 needs, *J. Geophys. Res.*, 104, 17661-17674, 1999.

1055

1056 Whipple, K. X., Forte, A. M., DiBiase, R. A., Gasparini, N. M., Ouimet, W. B.: Timescales of
1057 landscape response to divide migration and drainage capture: implications for the role of
1058 divide mobility in landscape evolution, *J. Geophys. Res.- Ea. Surf.*, 122, 248-273,
1059 <https://doi.org/10.1002/2016JF003973>, 2017.

1060

1061 Whitfield, E. and Harvey, A. M.: Interaction between the controls on fluvial system
1062 development: tectonics, climate, base level and river capture – Rio Alias, Southeast Spain, *Earth*
1063 *Surf. Process. Landforms*, 37, 1387-1397, <https://doi.org/10.1002/esp.3247>, 2012.

1064

1065 Willett, S. D.: Orogeny and orography: The effects of erosion on the structure of mountain belts,
1066 *J. Geophys. Res.*, 104, 28957-28981, 1999.

1067

1068 Willett, S. D., McCoy, S. W., Perron, J. T., Goren, L., and Chen, C. Y.: Dynamic reorganization
1069 of river basins, *Science*, 343, 1248765, <https://doi.org/10.1126/science.1248765>, 2014.

1070



1071 Wobus, C., Whipple, K. X., Kirby, E., Snyder, N., Johnson, J., Spyropolou, K., Crosby, B., and
1072 Sheehan, D.: Tectonics from topography: Procedures, promise, and pitfalls, in: Willett, S. D.,
1073 Hovius, N., Brandon, M. T., and Fisher, D. M. (Eds.): Tectonics, Climate, Landscape Evolution:
1074 Geological Society of America, Special Paper, 398, Penrose Conference Series, 55-74,
1075 [https://doi.org/10.1130/2006.2398\(04\)](https://doi.org/10.1130/2006.2398(04)), 2006.

1076

1077 Yang, R., Willett, S. D., and Goren, L.: In situ low-relief landscape formation as a result of river
1078 network disruption, *Nature*, 520, 526-529, <https://doi.org/10.1038/nature14354>, 2015.

1079

1080 Yanites, B. J., Elhers, T. A., Becker, J. K., Schnellmann, M., and Heuberger, S.: High magnitude
1081 and rapid incision from river capture: Rhine River, Switzerland, *J. Geophys. Res.- Ea. Surf.*,
1082 118, 1060-1084, <https://doi.org/10.1002/jgrf.20056>, 2013.

1083

1084

1085

1086

1087

1088

1089

1090

1091

1092

1093



Figure captions:

Figure 1: A) Topographic map of the Duero and Ebro basins and surrounding belts. B) Averaged topographic section throughout the Duero and Ebro basins showing important incision contrast between the two basins. The Duero basin recorded low incision, especially for its upper part, whereas the Ebro basin is highly excavated.

Figure 2: Simplified geological map of the study area.

Figure 3: Topographic map of the study area with all the rivers considered in this study. The red lines represent drainage divides between main hydrographic basins.

Figure 4: Zoom in the geological map of the Iberian Range showing the location of the Jalon river tributaries. The river long profiles of these streams and the location of knickpoints are shown to the left.

Figure 5: A) Zoom in the geological map of the Bureba sector. B) Zoom in the Homino river (Ebro tributary) capturing the upper reach of the Jordan river (Duero tributary). C) Schematic representation of this capture using river long profiles and map orientation, showing the associated knickpoint and wind gap.

Figure 6: Mean annual precipitation map for the study area obtained from Hijmans et al. (2005).

Figure 7: A) 3D topographic map of the Bureba sector showing important incision in the Ebro basin contrasting with the well-preserved Duero basin, and river capture evidences (elbows of capture, knickpoints and wind gaps). B) Google Earth image around the locality of Hontomin where the Homino river is capturing the upper reach of the Jordan river. C) and D) Remarkable wind gaps located on the Bureba anticline. Pictures have been taken from the north of this structure toward the south. E) Possible three steps evolution of the southwestward divide retreat through multiple river captures witnessed in the area.

Figure 8: River long profiles for all the streams described in the Bureba area showing remarkable evidences of river capture. Colors are given to rivers that are linked in these capture processes.



Figure 9: Topographic map showing the location of all the knickpoints and low relief surfaces that may be associated to river capture. The black dashed line represents a possible paleodrainage divide between the Ebro and Duero basins. The area between this dashed line and the present-day location of the divide in red may have belonged the Duero basin before being captured by the Ebro basin.

Figure 10: Topographic map with X values calculated on different opposite streams in the vicinity of the Ebro/Duero drainage divide. This map shows significant contrasting values between the Ebro and Duero drainage networks.

Figure 11: The Duero river long profile (black line) is compared to the difference between the specific stream power calculated for the possible ancient and for the present-day Duero river, in grey. Positive values suggest a diminution of the incision capacity of the Duero river, through time. Details on calculation are available in the Supplement (Section S1).

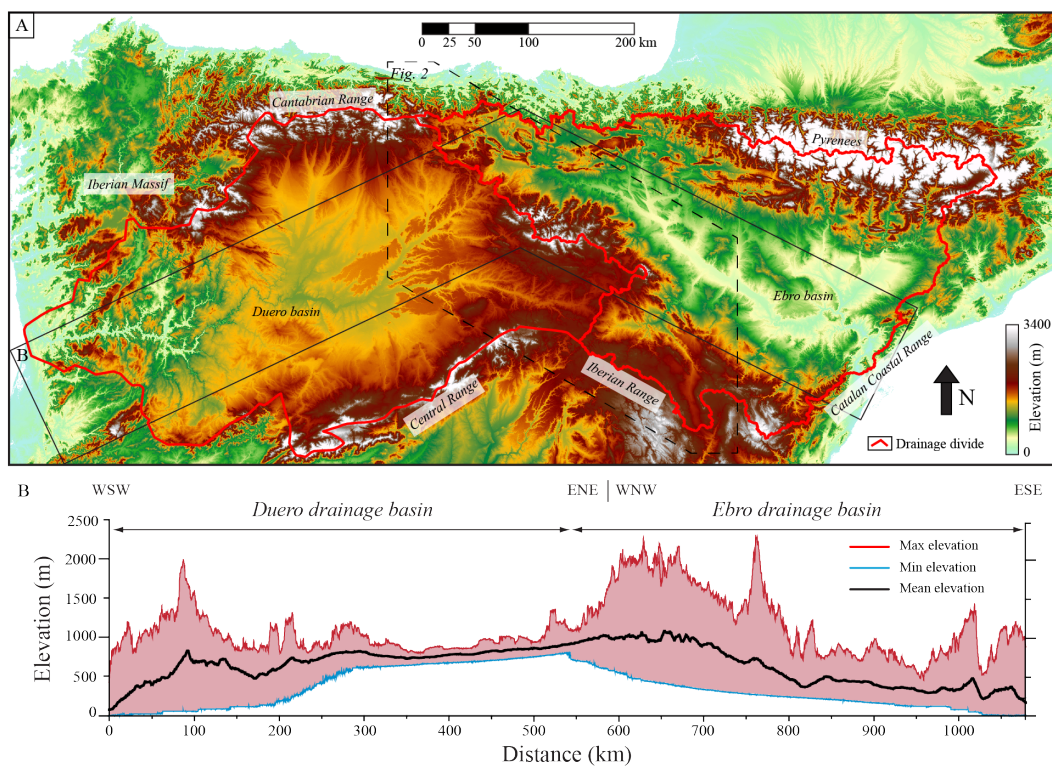


Figure 1

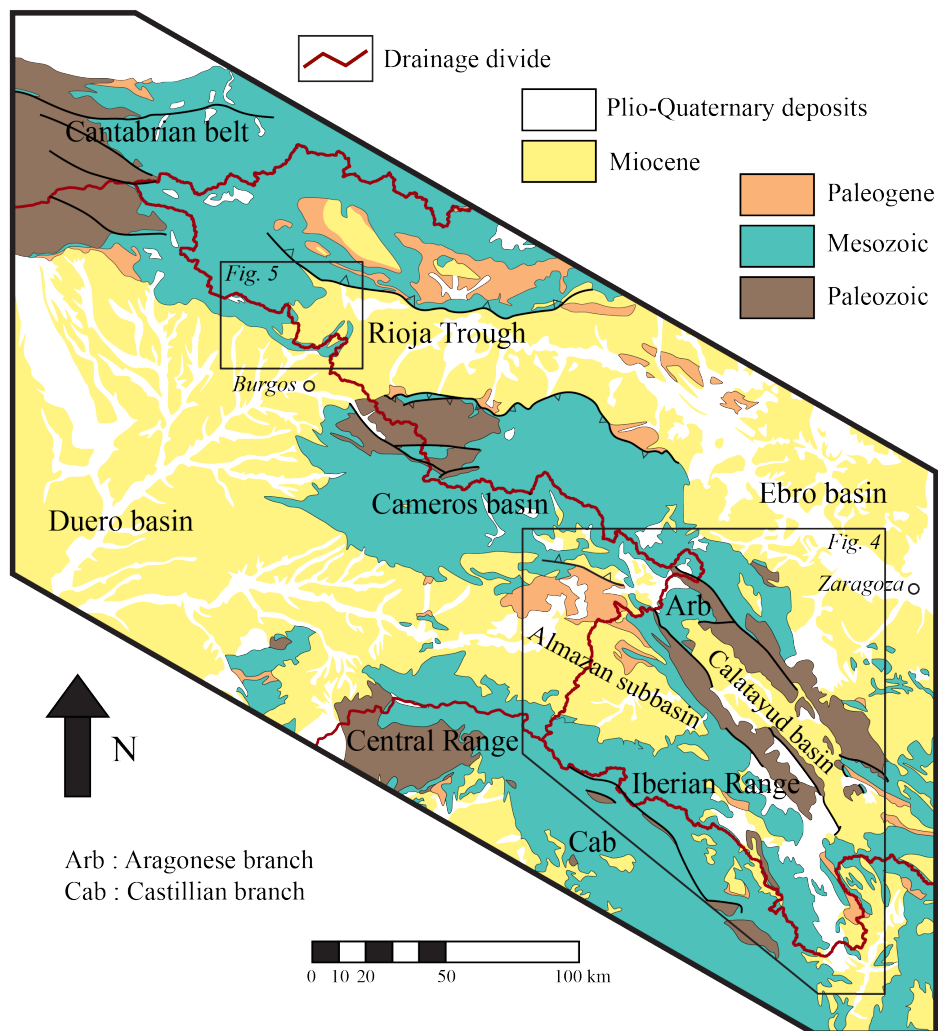


Figure 2

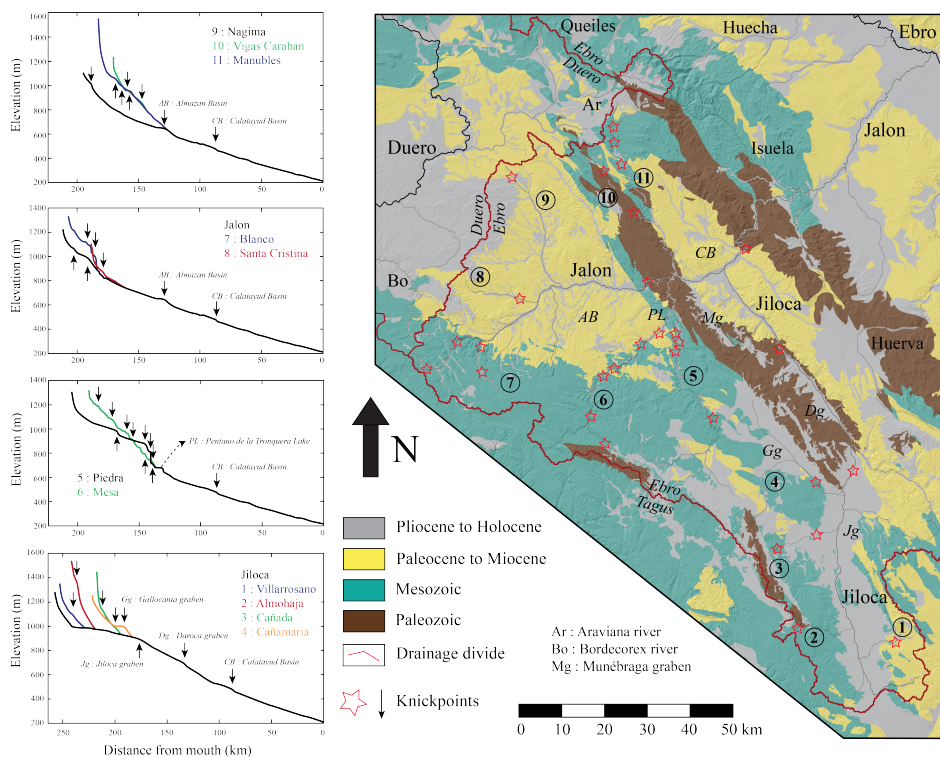


Figure 4

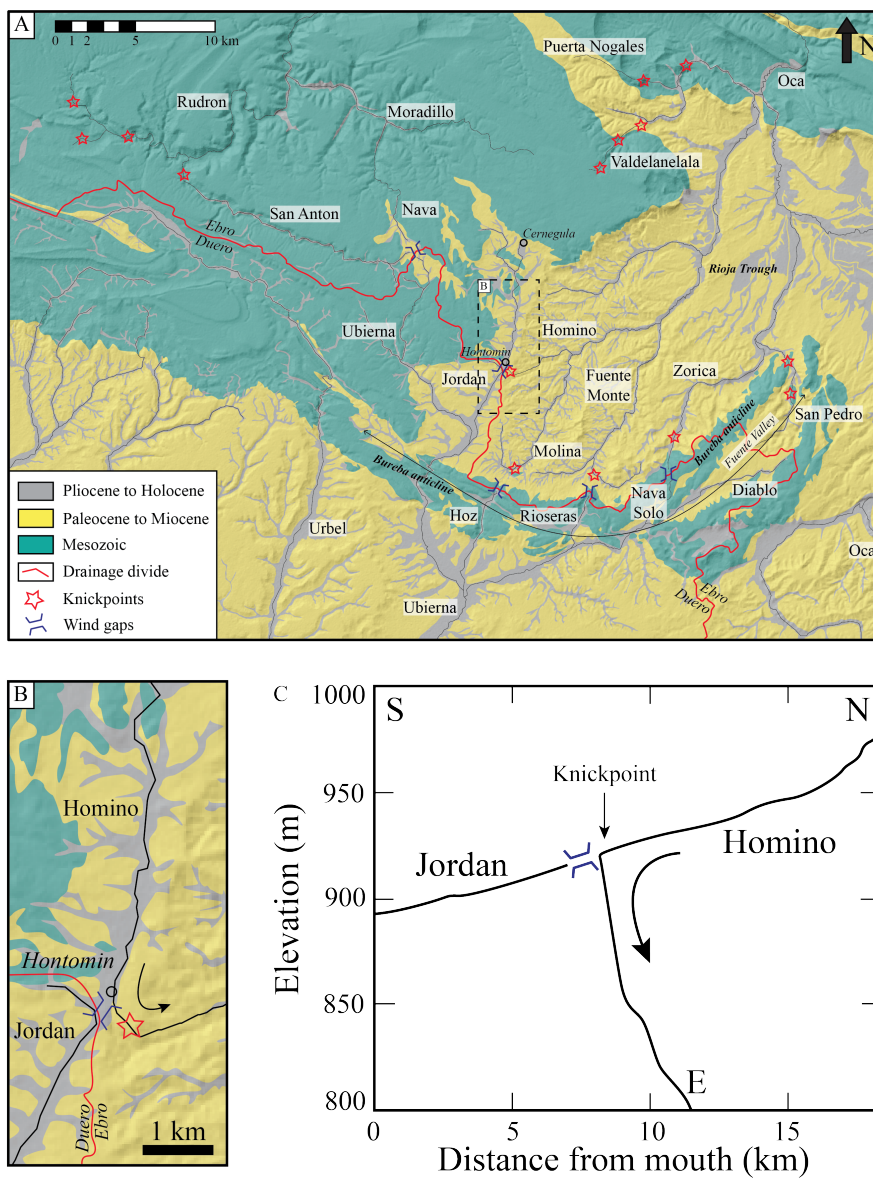


Figure 5

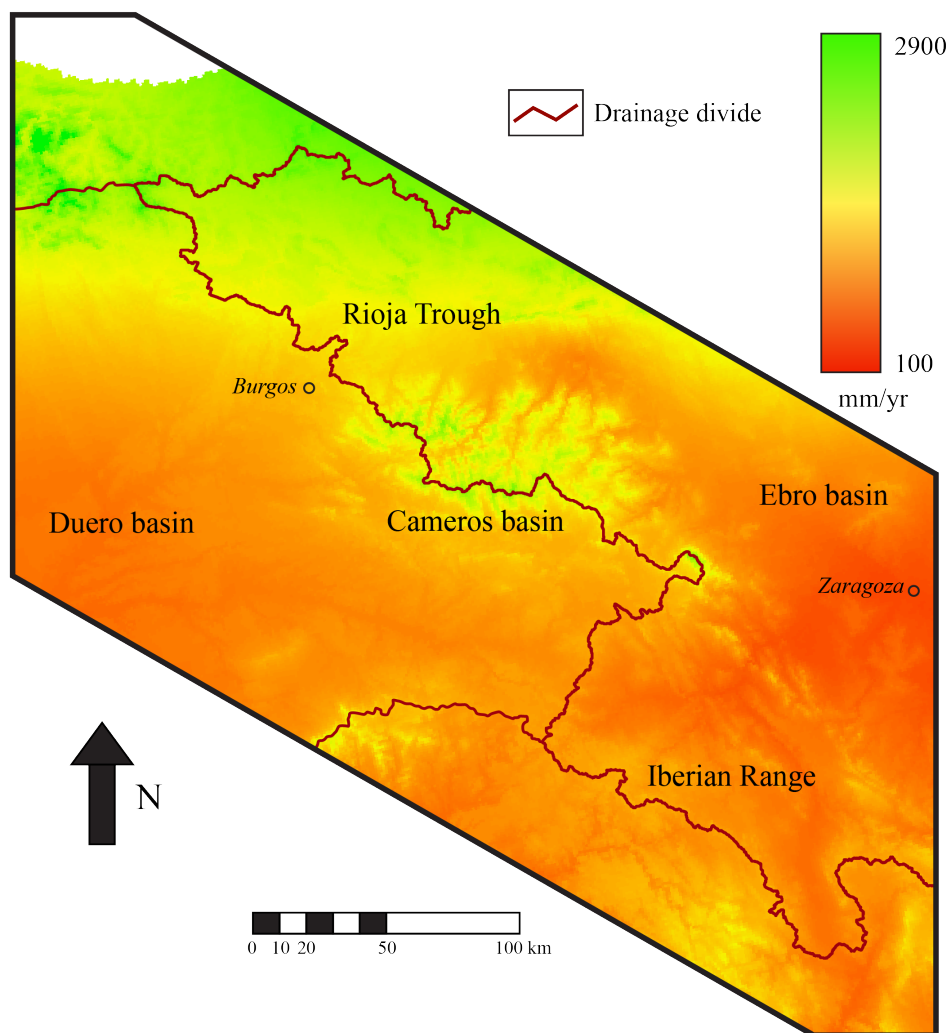


Figure 6

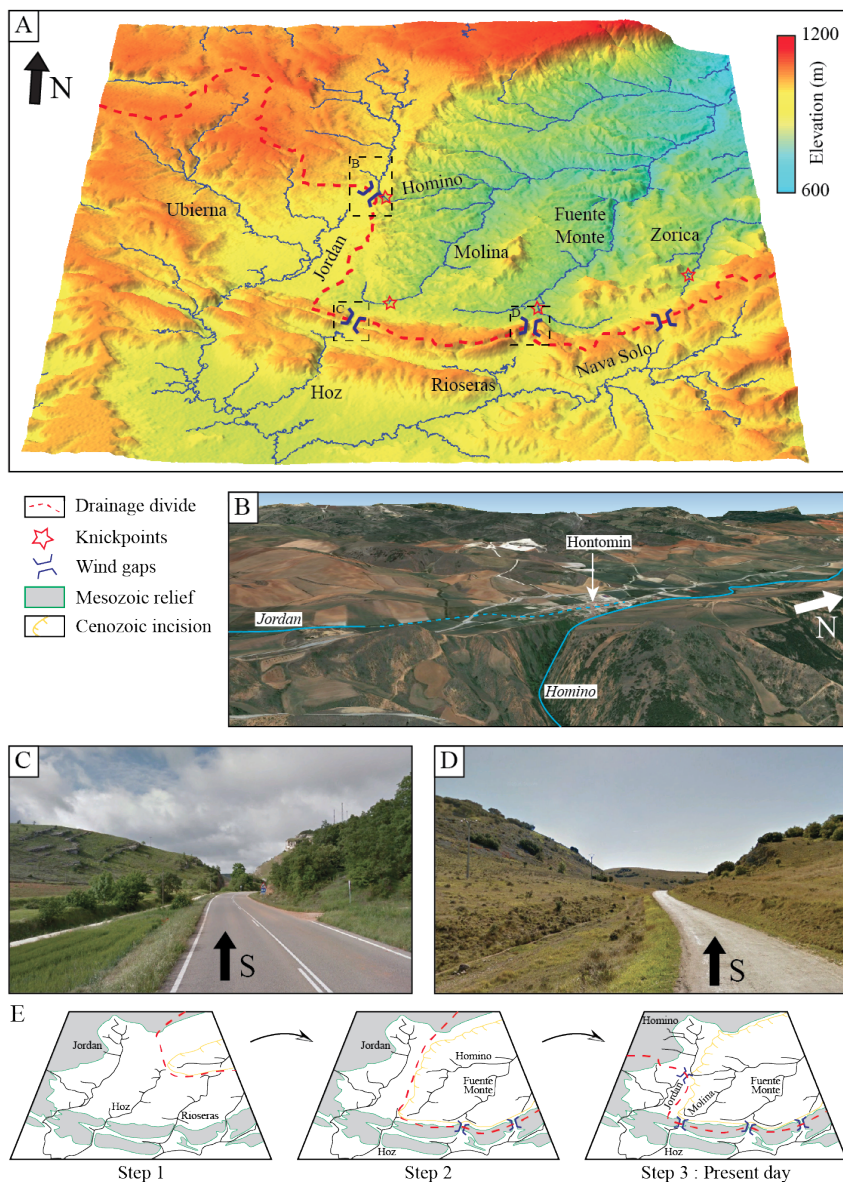


Figure 7

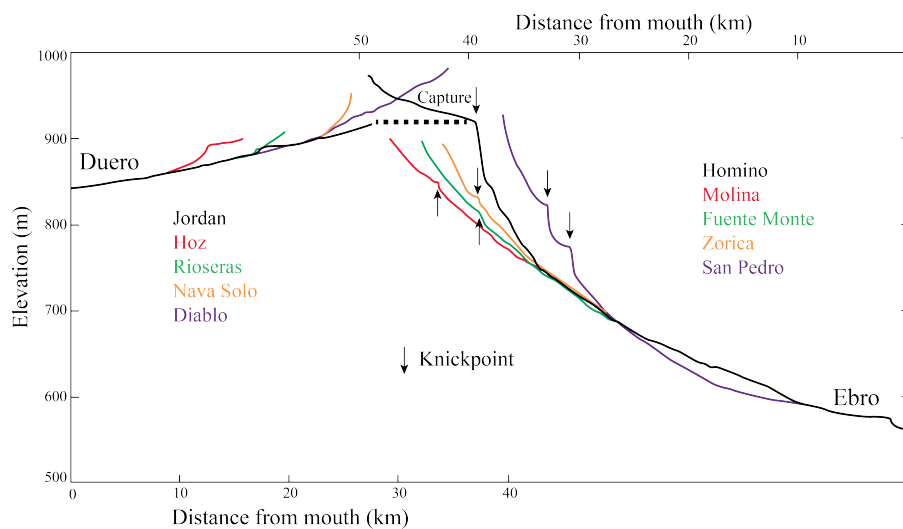


Figure 8

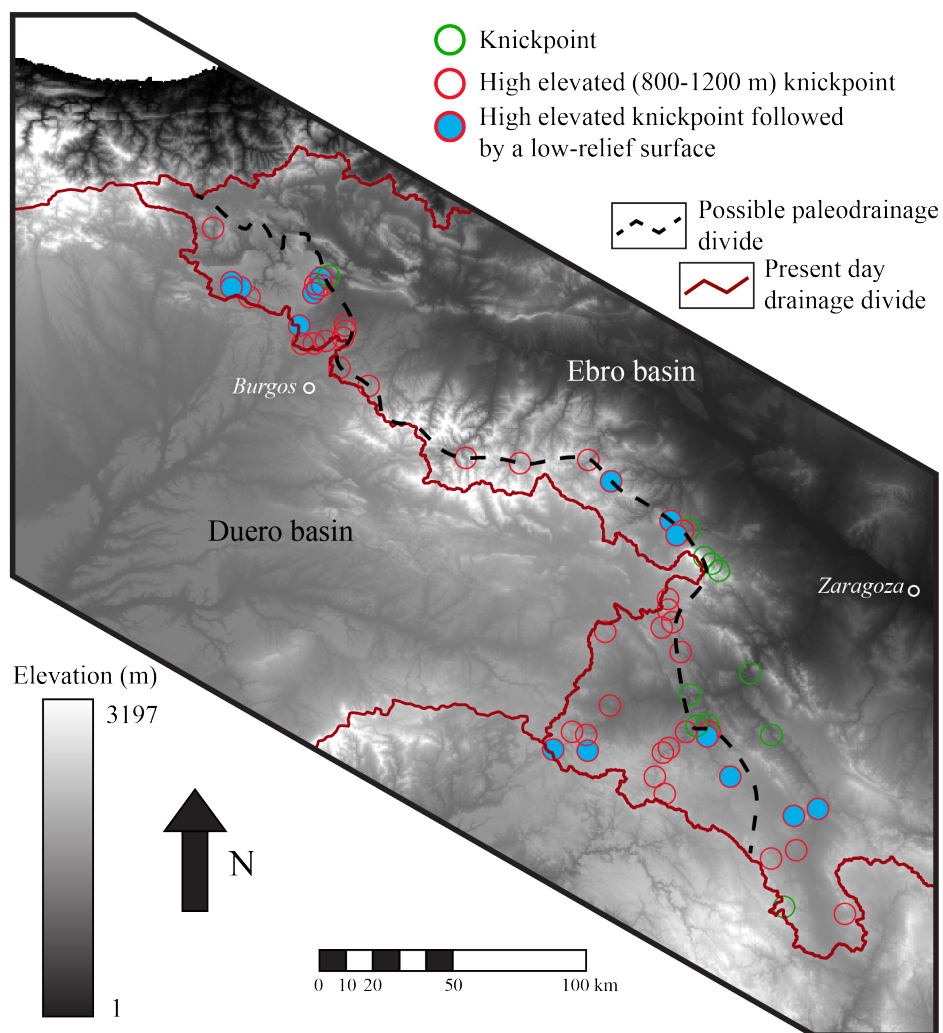


Figure 9

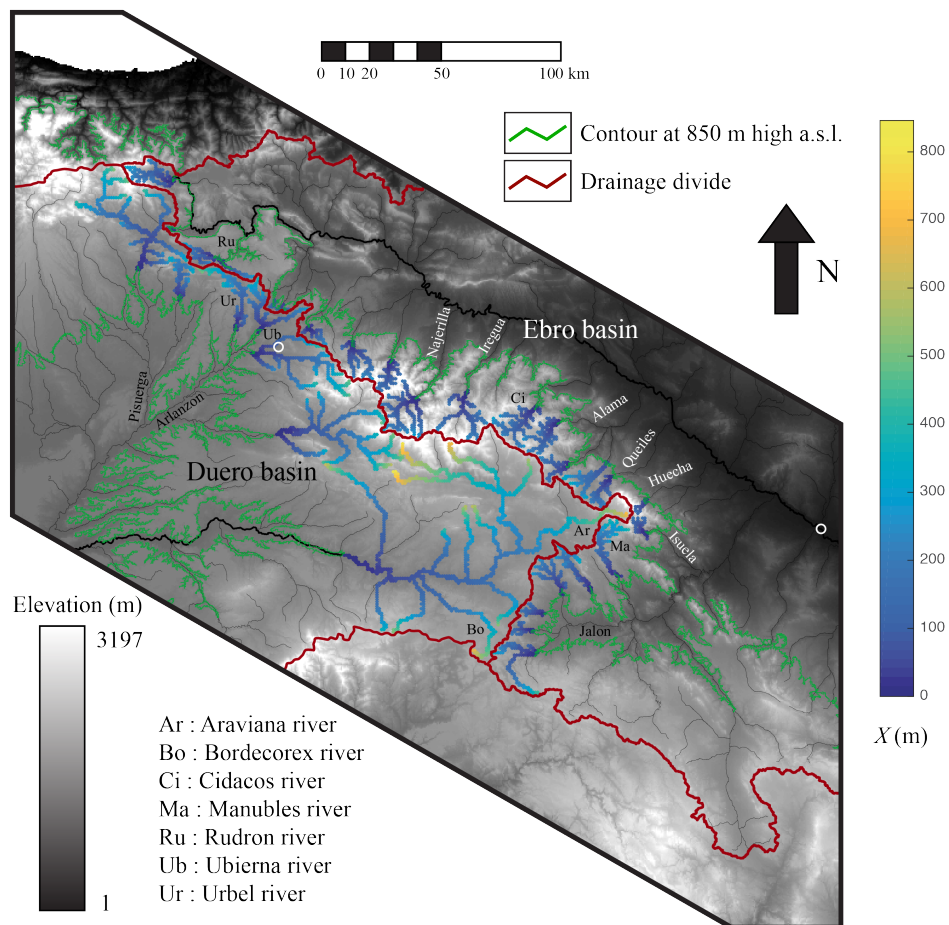


Figure 10

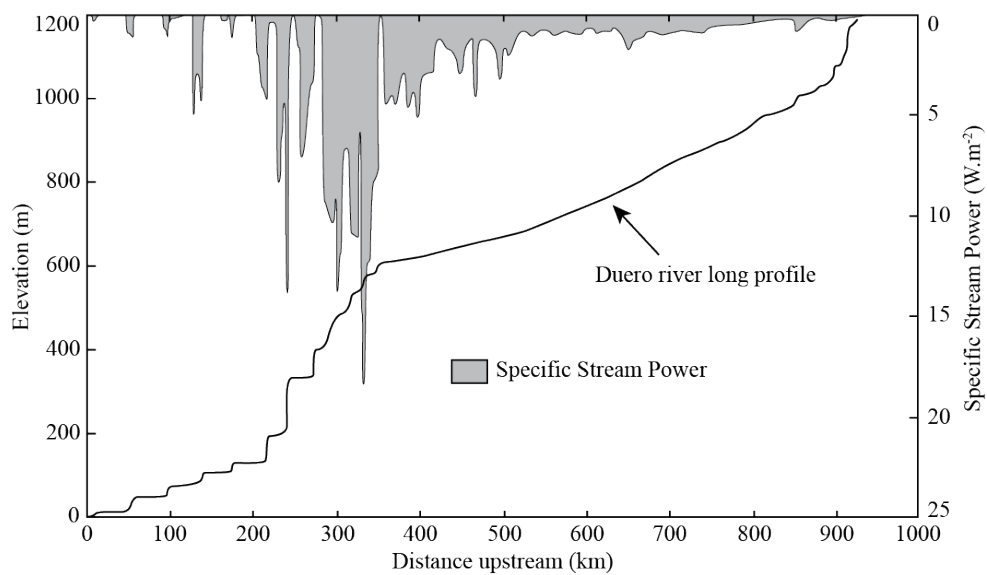


Figure 11